

# Integrable self-adaptive moving mesh schemes for multi-component short pulse type equations under general boundary conditions

Ayako Hori<sup>1</sup>, Ken-ichi Maruno<sup>2</sup>, Yasuhiro Ohta<sup>3</sup> and Bao-Feng Feng<sup>4</sup>

<sup>1</sup> Department of Pure and Applied Mathematics, School of Fundamental Science and Engineering, Waseda University, 3-4-1 Okubo, Shinjuku-ku, Tokyo 169-8555, Japan

<sup>2</sup> Department of Applied Mathematics, Faculty of Science and Engineering, Waseda University, 3-4-1 Okubo, Shinjuku-ku, Tokyo 169-8555, Japan

<sup>3</sup> Department of Mathematics, Kobe University, 1-1 Rokkodaicho, Nada-ku, Kobe 657-8501, Japan

<sup>4</sup> School of Mathematical and Statistical Sciences, The University of Texas Rio Grande Valley, 1201 West University Dr., Edinburg, Texas 78541, USA

E-mail: ayako0903@akane.waseda.jp kmaruno@waseda.jp  
ohta@math.kobe-u.ac.jp baofeng.feng@utrgv.edu

8 July 2025

**Abstract.** In this paper, we construct integrable self-adaptive moving mesh schemes for multi-component modified short pulse and short pulse equations under general boundary conditions including periodic boundary conditions by using the consistency condition with the hodograph transformation. We also construct multi-soliton solutions expressed by Pfaffian for our self-adaptive moving mesh schemes. Using self-adaptive moving mesh schemes presented in this paper, we perform numerical experiments to evaluate their effectiveness and accuracy as a numerical method.

*Keywords:* Self-adaptive moving mesh schemes, Multi-component short pulse type equations, General boundary conditions, Pfaffian

## 1. Introduction

The study of discrete integrable systems has been developed in connection with various fields of mathematics, physics, and engineering since the pioneering work by Hirota, Ablowitz-Ladik in the late 1970s [1, 2].

Hirota proposed a method for discretizing soliton equations while preserving their integrability based on bilinear equations and  $\tau$ -functions, and succeeded in discretizing various soliton equations such as the KdV equation and the sine-Gordon equation [3–7]. Furthermore, Ablowitz and Ladik proposed a method for discretizing soliton equations based on the Ablowitz-Kaup-Newell-Segur (AKNS) type linear eigenvalue problem for soliton equations, and succeeded in discretizing soliton equations such as the nonlinear Schrödinger equation while preserving its integrability [8–12].

It is known that there are soliton equations associated with Wadati-Konno-Ichikawa (WKI) type linear eigenvalue problems [13, 14]. Ishimori and Wadati-Sogo have shown that the soliton equations belonging to the WKI class can be transformed into the soliton equations associated with AKNS-type linear eigenvalue problems by hodograph transformations [15–18]. For a long time, integrable discretizations of soliton equations in the WKI class had been considered difficult. We succeeded in integrable discretizations of soliton equations associated with WKI-type linear eigenvalue problems by using the Hirota’s discretization method based on bilinear equations, which incorporates the idea of discretizing hodograph transformations [19–26]. We named their integrable discrete equations self-adaptive moving mesh schemes because the mesh spacing is automatically finely divided at large deformations when numerical computations are performed.

Integrable self-adaptive moving mesh schemes are difference schemes that automatically adjust the mesh spacing, which are obtained by discretizing integrable nonlinear wave equations with exact solutions such as loop and cusp soliton solutions in a way that preserves the structure of the exact solutions. The key to constructing a self-adaptive moving mesh scheme is the discretization of a hodograph transformation. It is well known that a hodograph transformation of a nonlinear wave equation corresponds to a conservation law [18]. In self-adaptive moving mesh schemes, a conserved density of a discrete conservation law corresponds to the mesh spacing. Therefore, the mesh spacing is automatically adjusted where the displacement changes rapidly.

It was reported that self-adaptive moving mesh schemes can also be derived as motions of discrete plane curves [27]. In terms of the geometric formulation, the Lagrangian representation of the evolution equation for the motion of a discrete curve is rewritten in the Eulerian representation by a discrete hodograph transformation, which is nothing but a self-adaptive moving mesh scheme.

Furthermore, it was reported that self-adaptive moving mesh schemes are effective and accurate in numerical computations [21, 24, 28]. However, all self-adaptive moving mesh schemes obtained so far have been constructed assuming boundary conditions with zero values at  $x \rightarrow \pm\infty$  on the infinite interval, i.e., the boundary conditions having ordinary soliton solutions. Therefore, when used as a numerical scheme, it was impossible to treat non-zero or periodic boundary conditions with non-zero values near the boundary. The difficulty in constructing self-adaptive moving mesh schemes under general boundary conditions is caused by the fact that the edge point of the discrete hodograph transformation moves when the value at the edge point is non-zero.

In this paper, we construct self-adaptive moving mesh schemes under general boundary conditions for the multi-component modified short pulse (MCmSP) equation [29]

$$u_{xt}^{(i)} = u^{(i)} + \left( \sum_{1 \leq j < k \leq n} c_{jk} u^{(j)} u^{(k)} u_x^{(i)} \right)_x - \left( \sum_{1 \leq j < k \leq n} c_{jk} u_x^{(j)} u_x^{(k)} \right) u^{(i)}, \quad i = 1, 2, \dots, n, \quad (1.1)$$

which is a multi-component generalization of the modified short pulse equation [30] and the

multi-component short pulse (MCSP) equation [31]

$$u_{xt}^{(i)} = u^{(i)} + \frac{1}{2} \left( \sum_{1 \leq j < k \leq n} c_{jk} u^{(j)} u^{(k)} u_x^{(i)} \right)_x, \quad i = 1, 2, \dots, n, \quad (1.2)$$

which is a multi-component generalization of the short pulse equation [32–36] by considering the consistency condition with the hodograph transformation. The coefficients  $c_{jk}$  are arbitrary constants with symmetry  $c_{jk} = c_{kj}$  ( $j, k = 1, 2, \dots, n$ ). We also construct multi-soliton solutions expressed by Pfaffian for our self-adaptive moving mesh schemes. Using the obtained self-adaptive moving mesh schemes, we perform numerical experiments to evaluate their effectiveness and accuracy as a numerical method.

This paper is structured as follows. In section 2, we describe the bilinear form of the MCmSP equation and its multi-soliton solution. In section 3, we construct a self-adaptive moving mesh scheme for the MCmSP equation under general boundary conditions, which has long been considered difficult. In section 4, we present the results of numerical simulations of the two-component modified short pulse (2-mSP) equation and the complex modified short pulse (CmSP) equation under the periodic boundary condition using the scheme constructed in the previous section. In sections 5 and 6, we discretize the MCSP equation and construct a self-adaptive moving mesh scheme for the MCSP equation under general boundary conditions, that has not been constructed before. In section 7, we perform numerical simulations of the two-component short pulse (2-SP) equation and the complex short pulse (CSP) equation under the periodic boundary condition. Finally, in section 8, we discuss the results and give conclusions.

## 2. Bilinear equations and N-soliton solution for the MCmSP equation

In this section, we describe the bilinear form and the hodograph transformation of the MCmSP equation

$$u_{xt}^{(i)} = u^{(i)} + \left( \sum_{1 \leq j < k \leq n} c_{jk} u^{(j)} u^{(k)} u_x^{(i)} \right)_x - \left( \sum_{1 \leq j < k \leq n} c_{jk} u_x^{(j)} u_x^{(k)} \right) u^{(i)}, \quad i = 1, 2, \dots, n, \quad (2.1)$$

and construct its N-soliton solution. First, by rewriting the MCmSP equation into the conservation law form

$$\left( \frac{1}{\rho} \right)_t - \left( \frac{F}{\rho} \right)_x = 0, \quad (2.2)$$

$$\rho = \left( 1 + \sum_{1 \leq j < k \leq n} c_{jk} u_x^{(j)} u_x^{(k)} \right)^{-1}, \quad F = \sum_{1 \leq j < k \leq n} c_{jk} u^{(j)} u^{(k)}, \quad (2.3)$$

the hodograph transformation

$$dX = \frac{1}{\rho} dx + \frac{F}{\rho} dt, \quad dT = dt, \quad (2.4)$$

is determined. From the hodograph transformation (2.4), we obtain the derivative law

$$\frac{\partial}{\partial X} = \rho \frac{\partial}{\partial x}, \quad \frac{\partial}{\partial T} = \frac{\partial}{\partial t} - F \frac{\partial}{\partial x}. \quad (2.5)$$

Next, transforming the MCmSP equation into

$$\partial_x \left( \partial_t - \sum_{1 \leq j < k \leq n} c_{jk} u^{(j)} u^{(k)} \partial_x \right) u^{(i)} = u^{(i)} \left( 2 - \left( 1 + \sum_{1 \leq j < k \leq n} c_{jk} u_x^{(j)} u_x^{(k)} \right) \right), \quad (2.6)$$

and applying the derivative law (2.5) and (2.3) to (2.6), we obtain

$$u_{XT}^{(i)} = u^{(i)} (2\rho - 1). \quad (2.7)$$

Furthermore, applying the derivative law (2.5) to the conservation law (2.2), we then have

$$\rho_T + \left( \sum_{1 \leq j < k \leq n} c_{jk} u^{(j)} u^{(k)} \right)_X = 0. \quad (2.8)$$

The equation (2.8) is the conservation law for  $X$  and  $T$ , where  $\rho$  is the conservation density and  $\sum_{1 \leq j < k \leq n} c_{jk} u^{(j)} u^{(k)}$  is the flux.

Therefore, the MCmSP equation (1.1) is transformed into the multi-component coupled integrable dispersionless (MCCID) equations

$$\begin{cases} u_{XT}^{(i)} = u^{(i)} (2\rho - 1), \\ \rho_T + \left( \sum_{1 \leq j < k \leq n} c_{jk} u^{(j)} u^{(k)} \right)_X = 0, \end{cases} \quad (2.9)$$

by the hodograph transformation (2.4).

Introducing the dependent variable transformation

$$u^{(i)} = \frac{g^{(i)}}{f} \quad (i = 1, 2, \dots, n), \quad \rho = 1 - (\log f)_{XT}, \quad (2.10)$$

the MCCID equations (2.9) lead to

$$\begin{cases} D_X D_T f \cdot g^{(i)} = f g^{(i)}, \\ D_T^2 f \cdot f = 2 \sum_{1 \leq j < k \leq n} c_{jk} g^{(j)} g^{(k)}, \end{cases} \quad (2.11)$$

where  $D_X$  and  $D_T$  are the Hirota's D-operators which are defined as

$$D_X^m D_T^n f(X, T) \cdot g(X, T) = \left( \frac{\partial}{\partial X} - \frac{\partial}{\partial X'} \right)^m \left( \frac{\partial}{\partial T} - \frac{\partial}{\partial T'} \right)^n f(X, T) g(X', T') \Big|_{X=X', T=T'}.$$

**Definition 2.1.** Let  $A$  be a  $2N \times 2N$  antisymmetric matrix defined by

$$A = (a_{i,j})_{1 \leq i, j \leq 2N},$$

where  $a_{i,j} = -a_{j,i}$  for  $i, j = 1, 2, \dots, 2N$ . The Pfaffian of  $A$  is defined by

$$\begin{aligned} \text{Pf}(A) &= \text{Pf}(a_{i,j})_{1 \leq i, j \leq 2N} = \text{Pf}(1, 2, \dots, 2N) \\ &= \sum_{\substack{i_1 < i_2 < \dots < i_N \\ i_1 < j_1 < i_2 < j_2 < \dots < i_N < j_N}} \text{sgn}(\pi) a_{i_1, j_1} a_{i_2, j_2} \cdots a_{i_N, j_N}, \end{aligned}$$

where  $\pi = \begin{pmatrix} 1 & 2 & \cdots & 2N-1 & 2N \\ i_1 & j_1 & \cdots & i_N & j_N \end{pmatrix}$  is a permutation of  $\{1, 2, \dots, 2N-1, 2N\}$ .

The Pfaffian is defined by the following expansion rule

$$\text{Pf}(1, 2, \dots, 2N) = \sum_{i=2}^{2N} (-1)^i \text{Pf}(1, i) \text{Pf}(2, 3, \dots, i-1, i+1, \dots, 2N-1, 2N).$$

For an antisymmetric matrix  $A$ , we have  $[\text{Pf}(A)]^2 = \det(A)$ .

**Lemma 2.2.** The bilinear equations (2.11) have the following Pfaffian solution:

$$f = \text{Pf}(a_1, \dots, a_{2N}, b_1, \dots, b_{2N}), \quad g^{(i)} = \text{Pf}(d_0, B_i, a_1, \dots, a_{2N}, b_1, \dots, b_{2N}), \quad (2.12)$$

where  $i = 1, 2, \dots, n$  and the elements of the Pfaffians are defined as

$$\text{Pf}(a_j, a_k) = \frac{p_j - p_k}{p_j + p_k} e^{\xi_j + \xi_k}, \quad \text{Pf}(a_j, b_k) = \delta_{j,k}, \quad (2.13)$$

$$\text{Pf}(b_j, b_k) = \frac{c_{\mu\nu}}{p_j^{-2} - p_k^{-2}} \quad (b_j \in B_\mu, b_k \in B_\nu), \quad (2.14)$$

$$\text{Pf}(d_l, a_k) = p_k^l e^{\xi_k}, \quad \text{Pf}(b_j, B_\mu) = \begin{cases} 1 & (b_j \in B_\mu) \\ 0 & (b_j \notin B_\mu) \end{cases}. \quad (2.15)$$

Here,  $j, k = 1, 2, \dots, 2N$ ,  $\mu, \nu = 1, 2, \dots, n$ ,  $\xi_j = p_j X + p_j^{-1} T + \xi_{i0}$  and  $l$  is an integer. A class of set  $B_\mu$  ( $\mu = 1, 2, \dots, n$ ) satisfies the following conditions

$$B_\mu \cap B_\nu = \emptyset \text{ if } \mu \neq \nu, \quad \cup_{\mu=1}^n B_\mu = \{b_1, b_2, \dots, b_{2N}\}. \quad (2.16)$$

The elements of the Pfaffians not defined above are defined as zero.

*Proof.* At first, we prove that the solutions (2.12) satisfy the first equation of the bilinear equation (2.11). As

$$\begin{aligned} \frac{\partial}{\partial X} \text{Pf}(a_j, a_k) &= (p_j - p_k) e^{\xi_j + \xi_k} = \text{Pf}(d_0, d_1, a_j, a_k), \\ \frac{\partial}{\partial T} \text{Pf}(a_j, a_k) &= (p_k^{-1} - p_j^{-1}) e^{\xi_j + \xi_k} = \text{Pf}(d_{-1}, d_0, a_j, a_k), \\ \frac{\partial^2}{\partial T^2} \text{Pf}(a_j, a_k) &= (p_k^{-2} - p_j^{-2}) e^{\xi_j + \xi_k} = \text{Pf}(d_{-2}, d_0, a_j, a_k), \\ \frac{\partial^2}{\partial X \partial T} \text{Pf}(a_j, a_k) &= (p_j p_k^{-1} - p_k p_j^{-1}) e^{\xi_j + \xi_k} = \text{Pf}(d_{-1}, d_1, a_j, a_k), \end{aligned}$$

we have

$$\begin{aligned} \frac{\partial f}{\partial X} &= \text{Pf}(d_0, d_1, \dots), & \frac{\partial f}{\partial T} &= \text{Pf}(d_{-1}, d_0, \dots), \\ \frac{\partial^2 f}{\partial T^2} &= \text{Pf}(d_{-2}, d_0, \dots), & \frac{\partial^2 f}{\partial X \partial T} &= \text{Pf}(d_{-1}, d_1, \dots). \end{aligned}$$

Here,  $\text{Pf}(d_i, d_j, a_1, \dots, a_{2N}, b_1, \dots, b_{2N})$  is denoted as  $\text{Pf}(d_i, d_j, \dots)$ .

Furthermore,

$$\begin{aligned}
\frac{\partial g^{(i)}}{\partial X} &= \frac{\partial}{\partial X} \left[ \sum_{j=1}^{2N} (-1)^j \text{Pf}(d_0, a_j) \text{Pf}(B_i, \dots, \hat{a}_j, \dots) \right] \\
&= \sum_{j=1}^{2N} (-1)^j [(\partial_X \text{Pf}(d_0, a_j)) \text{Pf}(B_i, \dots, \hat{a}_j, \dots) + \text{Pf}(d_0, a_j) \partial_X \text{Pf}(B_i, \dots, \hat{a}_j, \dots)] \\
&= \sum_{j=1}^{2N} (-1)^j [\text{Pf}(d_1, a_j) \text{Pf}(B_i, \dots, \hat{a}_j, \dots) + \text{Pf}(d_0, a_j) \text{Pf}(d_0, d_1, B_i, \dots, \hat{a}_j, \dots)] \\
&= \text{Pf}(d_1, B_i, \dots) + \text{Pf}(d_0, d_0, d_1, B_i, \dots) \\
&= \text{Pf}(d_1, B_i, \dots).
\end{aligned}$$

Similarly, we have

$$\begin{aligned}
\frac{\partial g^{(i)}}{\partial T} &= \frac{\partial}{\partial T} \left[ \sum_{j=1}^{2N} (-1)^j \text{Pf}(d_0, a_j) \text{Pf}(B_i, \dots, \hat{a}_j, \dots) \right] \\
&= \sum_{j=1}^{2N} (-1)^j [(\partial_T \text{Pf}(d_0, a_j)) \text{Pf}(B_i, \dots, \hat{a}_j, \dots) + \text{Pf}(d_0, a_j) \partial_T \text{Pf}(B_i, \dots, \hat{a}_j, \dots)] \\
&= \sum_{j=1}^{2N} (-1)^j [\text{Pf}(d_{-1}, a_j) \text{Pf}(B_i, \dots, \hat{a}_j, \dots) + \text{Pf}(d_0, a_j) \text{Pf}(d_{-1}, d_0, B_i, \dots, \hat{a}_j, \dots)] \\
&= \text{Pf}(d_{-1}, B_i, \dots) + \text{Pf}(d_0, d_{-1}, d_0, B_i, \dots) \\
&= \text{Pf}(d_{-1}, B_i, \dots), \\
\frac{\partial^2 g^{(i)}}{\partial X \partial T} &= \frac{\partial}{\partial X} \left[ \sum_{j=1}^{2N} (-1)^j \text{Pf}(d_{-1}, a_j) \text{Pf}(B_i, \dots, \hat{a}_j, \dots) \right] \\
&= \sum_{j=1}^{2N} (-1)^j [(\partial_X \text{Pf}(d_{-1}, a_j)) \text{Pf}(B_i, \dots, \hat{a}_j, \dots) + \text{Pf}(d_{-1}, a_j) \partial_X \text{Pf}(B_i, \dots, \hat{a}_j, \dots)] \\
&= \sum_{j=1}^{2N} (-1)^j [\text{Pf}(d_0, a_j) \text{Pf}(B_i, \dots, \hat{a}_j, \dots) + \text{Pf}(d_{-1}, a_j) \text{Pf}(d_0, d_1, B_i, \dots, \hat{a}_j, \dots)] \\
&= \text{Pf}(d_0, B_i, \dots) + \text{Pf}(d_{-1}, d_0, d_1, B_i, \dots) \\
&= \text{Pf}(d_0, B_i, \dots) + \text{Pf}(d_{-1}, B_i, d_0, d_1, \dots).
\end{aligned}$$

An algebraic identity of Pfaffian [38]

$$\begin{aligned}
\text{Pf}(d_{-1}, B_i, d_0, d_1, \dots) \text{Pf}(\dots) &= \text{Pf}(d_{-1}, d_0, \dots) \text{Pf}(d_1, B_i, \dots) \\
&\quad - \text{Pf}(d_{-1}, d_1, \dots) \text{Pf}(d_0, B_i, \dots) + \text{Pf}(d_{-1}, B_i, \dots) \text{Pf}(d_0, d_1, \dots)
\end{aligned}$$

leads to

$$(\partial_X \partial_T g^{(i)} - g^{(i)}) \times f = \partial_T f \times \partial_X g^{(i)} - \partial_X \partial_T f \times g^{(i)} + \partial_T g^{(i)} \times \partial_X f,$$

which is the first equation of the bilinear equations (2.11).

Next, we prove that the solutions (2.12) satisfy the second equation of the bilinear equation (2.11). The right-hand side of the second equation of the bilinear equation (2.11) leads to

$$\begin{aligned}
2 \sum_{1 \leq \mu < \nu \leq n} c_{\mu\nu} g^{(\mu)} g^{(\nu)} &= \sum_{1 \leq \mu, \nu \leq n} c_{\mu\nu} \text{Pf}(d_0, B_\mu, \dots) \text{Pf}(d_0, B_\nu, \dots) \\
&= \sum_{1 \leq \mu, \nu \leq n} c_{\mu\nu} \sum_{j,k}^{2N} (-1)^{j+k} \text{Pf}(B_\mu, b_j) \text{Pf}(d_0, \dots, \hat{b}_j, \dots) \text{Pf}(B_\nu, b_k) \text{Pf}(d_0, \dots, \hat{b}_k, \dots) \\
&= \sum_{j,k}^{2N} (-1)^{j+k} \sum_{1 \leq \mu, \nu \leq n} c_{\mu\nu} \text{Pf}(B_\mu, b_j) \text{Pf}(B_\nu, b_k) \text{Pf}(d_0, \dots, \hat{b}_j, \dots) \text{Pf}(d_0, \dots, \hat{b}_k, \dots) \\
&= \sum_{j,k}^{2N} (-1)^{j+k} (p_j^{-2} - p_k^{-2}) \text{Pf}(b_j, b_k) \text{Pf}(d_0, \dots, \hat{b}_j, \dots) \text{Pf}(d_0, \dots, \hat{b}_k, \dots). \tag{2.17}
\end{aligned}$$

Now, expanding  $\text{Pf}(b_j, d_0, \dots)$  which is trivially zero Pfaffian, we obtain

$$\sum_{k=1}^{2N} (-1)^{j+k} \text{Pf}(b_j, b_k) \text{Pf}(d_0, \dots, \hat{b}_k, \dots) = \text{Pf}(d_0, \dots, \hat{a}_j, \dots),$$

which leads to

$$\begin{aligned}
&\sum_{j,k}^{2N} (-1)^{j+k} p_j^{-2} \text{Pf}(b_j, b_k) \text{Pf}(d_0, \dots, \hat{b}_j, \dots) \text{Pf}(d_0, \dots, \hat{b}_k, \dots) \\
&= \sum_j^{2N} p_j^{-2} \text{Pf}(d_0, \dots, \hat{a}_j, \dots) \text{Pf}(d_0, \dots, \hat{b}_j, \dots). \tag{2.18}
\end{aligned}$$

Similarly, we have

$$\begin{aligned}
&-\sum_{j,k}^{2N} (-1)^{j+k} p_k^{-2} \text{Pf}(b_j, b_k) \text{Pf}(d_0, \dots, \hat{b}_j, \dots) \text{Pf}(d_0, \dots, \hat{b}_k, \dots) \\
&= \sum_k^{2N} p_k^{-2} \text{Pf}(d_0, \dots, \hat{a}_k, \dots) \text{Pf}(d_0, \dots, \hat{b}_k, \dots). \tag{2.19}
\end{aligned}$$

Substituting (2.18) and (2.19) into (2.17), we then have

$$\sum_{1 \leq \mu < \nu \leq n} c_{\mu\nu} g^{(\mu)} g^{(\nu)} = \sum_j^{2N} p_j^{-2} \text{Pf}(d_0, \dots, \hat{a}_j, \dots) \text{Pf}(d_0, \dots, \hat{b}_j, \dots). \tag{2.20}$$

Next, the following equation gives

$$\begin{aligned}
\frac{\partial^2 f}{\partial T^2} \times 0 - \frac{\partial f}{\partial T} \frac{\partial f}{\partial T} &= \text{Pf}(d_{-2}, d_0, \dots) \text{Pf}(d_0, d_0, \dots) - \text{Pf}(d_{-1}, d_0, \dots) \text{Pf}(d_{-1}, d_0, \dots) \\
&= \sum_{j=1}^{2N} (-1)^j \text{Pf}(d_{-2}, a_j) \text{Pf}(d_0, \dots, \hat{a}_j, \dots) \sum_{k=1}^{2N} (-1)^k \text{Pf}(d_0, a_k) \text{Pf}(d_0, \dots, \hat{a}_k, \dots)
\end{aligned}$$

$$\begin{aligned}
& - \sum_{j=1}^{2N} (-1)^j \text{Pf}(d_{-1}, a_j) \text{Pf}(d_0, \dots, \hat{a}_j, \dots) \sum_{k=1}^{2N} (-1)^k \text{Pf}(d_{-1}, a_k) \text{Pf}(d_0, \dots, \hat{a}_k, \dots) \\
&= \sum_{j,k=1}^{2N} (-1)^{j+k} [\text{Pf}(d_{-2}, a_j) \text{Pf}(d_0, a_k) - \text{Pf}(d_{-1}, a_j) \text{Pf}(d_{-1}, a_k)] \\
&\quad \times \text{Pf}(d_0, \dots, \hat{a}_j, \dots) \text{Pf}(d_0, \dots, \hat{a}_k, \dots) \\
&= \sum_{j,k=1}^{2N} (-1)^{j+k+1} (p_j^{-2} + p_j^{-1} p_k^{-1}) \text{Pf}(a_j, a_k) \text{Pf}(d_0, \dots, \hat{a}_j, \dots) \text{Pf}(d_0, \dots, \hat{a}_k, \dots). \tag{2.21}
\end{aligned}$$

Since

$$\begin{aligned}
& \sum_{j,k=1}^{2N} (-1)^{j+k+1} p_j^{-1} p_k^{-1} \text{Pf}(a_j, a_k) \text{Pf}(d_0, \dots, \hat{a}_j, \dots) \text{Pf}(d_0, \dots, \hat{a}_k, \dots) \\
&= \sum_{k,j=1}^{2N} (-1)^{k+j+1} p_k^{-1} p_j^{-1} \text{Pf}(a_k, a_j) \text{Pf}(d_0, \dots, \hat{a}_k, \dots) \text{Pf}(d_0, \dots, \hat{a}_j, \dots) \\
&= - \sum_{j,k=1}^{2N} (-1)^{j+k+1} p_j^{-1} p_k^{-1} \text{Pf}(a_j, a_k) \text{Pf}(d_0, \dots, \hat{a}_j, \dots) \text{Pf}(d_0, \dots, \hat{a}_k, \dots), \tag{2.22}
\end{aligned}$$

we obtain

$$\sum_{j,k=1}^{2N} (-1)^{j+k+1} p_j^{-1} p_k^{-1} \text{Pf}(a_j, a_k) \text{Pf}(d_0, \dots, \hat{a}_j, \dots) \text{Pf}(d_0, \dots, \hat{a}_k, \dots) = 0. \tag{2.23}$$

Substituting (2.23) into (2.21), it follows

$$\begin{aligned}
& - \frac{\partial f}{\partial T} \frac{\partial f}{\partial T} = \sum_{j,k=1}^{2N} (-1)^{j+k+1} p_j^{-2} \text{Pf}(a_j, a_k) \text{Pf}(d_0, \dots, \hat{a}_j, \dots) \text{Pf}(d_0, \dots, \hat{a}_k, \dots) \\
&= \sum_{j=1}^{2N} (-1)^{j+1} p_j^{-2} \text{Pf}(d_0, \dots, \hat{a}_j, \dots) \left[ \sum_{k=1}^{2N} (-1)^k \text{Pf}(a_j, a_k) \text{Pf}(d_0, \dots, \hat{a}_k, \dots) \right]. \tag{2.24}
\end{aligned}$$

Now, expanding  $\text{Pf}(a_j, d_0, \dots)$  which is trivially zero Pfaffian, we obtain

$$\sum_{k=1}^{2N} (-1)^k \text{Pf}(a_j, a_k) \text{Pf}(d_0, \dots, \hat{a}_k, \dots) = \text{Pf}(d_0, a_j) \text{Pf}(\dots) + (-1)^{j+1} \text{Pf}(d_0, \dots, \hat{b}_j, \dots). \tag{2.25}$$

Substituting (2.25) into (2.24), we have

$$\begin{aligned}
& - \frac{\partial f}{\partial T} \frac{\partial f}{\partial T} = \sum_{j=1}^{2N} (-1)^{j+1} p_j^{-2} \text{Pf}(d_0, \dots, \hat{a}_j, \dots) \left[ \text{Pf}(d_0, a_j) \text{Pf}(\dots) + (-1)^{j+1} \text{Pf}(d_0, \dots, \hat{b}_j, \dots) \right] \\
&= \sum_{j=1}^{2N} (-1)^{j+1} p_j^{-2} \text{Pf}(d_0, a_j) \text{Pf}(d_0, \dots, \hat{a}_j, \dots) \text{Pf}(\dots)
\end{aligned}$$

$$\begin{aligned}
& + \sum_{j=1}^{2N} p_j^{-2} \text{Pf}(d_0, \dots, \hat{a}_j, \dots) \text{Pf}(d_0, \dots, \hat{b}_j, \dots) \\
= & - \sum_{j=1}^{2N} (-1)^j p_j^{-2} \text{Pf}(d_0, a_j) \text{Pf}(d_0, \dots, \hat{a}_j, \dots) \text{Pf}(\dots) \\
& + \sum_{j=1}^{2N} p_j^{-2} \text{Pf}(d_0, \dots, \hat{a}_j, \dots) \text{Pf}(d_0, \dots, \hat{b}_j, \dots) \\
= & - \sum_{j=1}^{2N} (-1)^j \text{Pf}(d_{-2}, a_j) \text{Pf}(d_0, \dots, \hat{a}_j, \dots) \text{Pf}(\dots) \\
& + \sum_{j=1}^{2N} p_j^{-2} \text{Pf}(d_0, \dots, \hat{a}_j, \dots) \text{Pf}(d_0, \dots, \hat{b}_j, \dots) \\
= & - \text{Pf}(d_{-2}, d_0, \dots) \text{Pf}(\dots) + \sum_{j=1}^{2N} p_j^{-2} \text{Pf}(d_0, \dots, \hat{a}_j, \dots) \text{Pf}(d_0, \dots, \hat{b}_j, \dots) \\
= & - \frac{\partial^2 f}{\partial T^2} f + \sum_{1 \leq \mu < \nu \leq n} c_{\mu\nu} g^{(\mu)} g^{(\nu)}.
\end{aligned}$$

The last calculation used (2.20). Therefore, we arrive at

$$\frac{\partial^2 f}{\partial T^2} f - \frac{\partial f}{\partial T} \frac{\partial f}{\partial T} = \sum_{1 \leq \mu < \nu \leq n} c_{\mu\nu} g^{(\mu)} g^{(\nu)},$$

which is the second equation of the bilinear equations (2.11).  $\square$

**Example 2.3.** 1-soliton : For  $N = 1, n = 2, B_1 = \{b_1\}, B_2 = \{b_2\}, c_{12} = 1$ , we obtain the  $\tau$ -functions  $f, g^{(1)}$  and  $g^{(2)}$  as follows:

$$\begin{aligned}
f &= \text{Pf}(a_1, a_2, b_1, b_2) \\
&= \text{Pf}(a_1, a_2) \text{Pf}(b_1, b_2) - \text{Pf}(a_1, b_1) \text{Pf}(a_2, b_2) + \text{Pf}(a_1, b_2) \text{Pf}(a_2, b_1) \\
&= \frac{p_1 - p_2}{p_1 + p_2} \frac{1}{p_1^{-2} - p_2^{-2}} e^{\xi_1 + \xi_2} - 1 = -1 - b_{12} e^{\xi_1 + \xi_2}, \\
g^{(1)} &= \text{Pf}(d_0, B_1, a_1, a_2, b_1, b_2) \\
&= \text{Pf}(d_0, B_1) \text{Pf}(a_1, a_2, b_1, b_2) - \text{Pf}(d_0, a_1) \text{Pf}(B_1, a_2, b_1, b_2) + \text{Pf}(d_0, a_2) \text{Pf}(B_1, a_1, b_1, b_2) \\
&\quad - \text{Pf}(d_0, b_1) \text{Pf}(B_1, a_1, a_2, b_2) + \text{Pf}(d_0, b_2) \text{Pf}(B_1, a_1, a_2, b_1) \\
&= \text{Pf}(d_0, B_1) (\text{Pf}(a_1, a_2) \text{Pf}(b_1, b_2) - \text{Pf}(a_1, b_1) \text{Pf}(a_2, b_2) + \text{Pf}(a_1, b_2) \text{Pf}(a_2, b_1)) \\
&\quad - \text{Pf}(d_0, a_1) (\text{Pf}(B_1, a_2) \text{Pf}(b_1, b_2) - \text{Pf}(B_1, b_1) \text{Pf}(a_2, b_2) + \text{Pf}(B_1, b_2) \text{Pf}(a_2, b_1)) \\
&\quad + \text{Pf}(d_0, a_2) (\text{Pf}(B_1, a_1) \text{Pf}(b_1, b_2) - \text{Pf}(B_1, b_1) \text{Pf}(a_1, b_2) + \text{Pf}(B_1, b_2) \text{Pf}(a_1, b_1)) \\
&\quad - \text{Pf}(d_0, b_1) (\text{Pf}(B_1, a_1) \text{Pf}(a_2, b_2) - \text{Pf}(B_1, a_2) \text{Pf}(a_1, b_2) + \text{Pf}(B_1, b_2) \text{Pf}(a_1, a_2)) \\
&\quad + \text{Pf}(d_0, b_2) (\text{Pf}(B_1, a_1) \text{Pf}(a_2, b_1) - \text{Pf}(B_1, a_2) \text{Pf}(a_1, b_1) + \text{Pf}(B_1, b_1) \text{Pf}(a_1, a_2)) \\
&= -e^{\xi_1}, \\
g^{(2)} &= \text{Pf}(d_0, B_2, a_1, a_2, b_1, b_2)
\end{aligned}$$

$$\begin{aligned}
&= \text{Pf}(d_0, B_2)\text{Pf}(a_1, a_2, b_1, b_2) - \text{Pf}(d_0, a_1)\text{Pf}(B_2, a_2, b_1, b_2) + \text{Pf}(d_0, a_2)\text{Pf}(B_2, a_1, b_1, b_2) \\
&\quad - \text{Pf}(d_0, b_1)\text{Pf}(B_2, a_1, a_2, b_2) + \text{Pf}(d_0, b_2)\text{Pf}(B_2, a_1, a_2, b_1) \\
&= \text{Pf}(d_0, B_2) (\text{Pf}(a_1, a_2)\text{Pf}(b_1, b_2) - \text{Pf}(a_1, b_1)\text{Pf}(a_2, b_2) + \text{Pf}(a_1, b_2)\text{Pf}(a_2, b_1)) \\
&\quad - \text{Pf}(d_0, a_1) (\text{Pf}(B_2, a_2)\text{Pf}(b_1, b_2) - \text{Pf}(B_2, b_1)\text{Pf}(a_2, b_2) + \text{Pf}(B_2, b_2)\text{Pf}(a_2, b_1)) \\
&\quad + \text{Pf}(d_0, a_2) (\text{Pf}(B_2, a_1)\text{Pf}(b_1, b_2) - \text{Pf}(B_2, b_1)\text{Pf}(a_1, b_2) + \text{Pf}(B_2, b_2)\text{Pf}(a_1, b_1)) \\
&\quad - \text{Pf}(d_0, b_1) (\text{Pf}(B_2, a_1)\text{Pf}(a_2, b_2) - \text{Pf}(B_2, a_2)\text{Pf}(a_1, b_2) + \text{Pf}(B_2, b_2)\text{Pf}(a_1, a_2)) \\
&\quad + \text{Pf}(d_0, b_2) (\text{Pf}(B_2, a_1)\text{Pf}(a_2, b_1) - \text{Pf}(B_2, a_2)\text{Pf}(a_1, b_1) + \text{Pf}(B_2, b_1)\text{Pf}(a_1, a_2)) \\
&= -e^{\xi_2},
\end{aligned}$$

where  $b_{jk} = \left(\frac{p_j p_k}{p_j + p_k}\right)^2$  and  $\xi_j = p_j X + \frac{1}{p_j} T + \xi_{j0}$ .

Letting  $\xi_{j0} = \xi'_{j0} + \log a_j$ , the  $\tau$ -function can be rewritten as

$$f = -1 - a_1 a_2 b_{12} e^{\eta_1 + \eta_2}, \quad g^{(1)} = -a_1 e^{\eta_1}, \quad g^{(2)} = -a_2 e^{\eta_2}. \quad (2.26)$$

where  $b_{jk} = \left(\frac{p_j p_k}{p_j + p_k}\right)^2$  and  $\eta_j = p_j X + \frac{1}{p_j} T + \xi'_{j0}$ .

2-soliton : For  $N = 2, n = 2, B_1 = \{b_1, b_2\}, B_2 = \{b_3, b_4\}, c_{12} = 1$ . If a term contains a Pfaffian with zero elements, we omit that term. By the expansion rule, we obtain the  $\tau$ -function  $f$  as follows:

$$\begin{aligned}
f &= \text{Pf}(a_1, a_2, a_3, a_4, b_1, b_2, b_3, b_4) \\
&= \text{Pf}(a_1, a_2)\text{Pf}(a_3, a_4, b_1, b_2, b_3, b_4) - \text{Pf}(a_1, a_3)\text{Pf}(a_2, a_4, b_1, b_2, b_3, b_4) \\
&\quad + \text{Pf}(a_1, a_4)\text{Pf}(a_2, a_3, b_1, b_2, b_3, b_4) - \text{Pf}(a_1, b_1)\text{Pf}(a_2, a_3, a_4, b_2, b_3, b_4) \\
&\quad + \text{Pf}(a_1, b_2)\text{Pf}(a_2, a_3, a_4, b_1, b_3, b_4) - \text{Pf}(a_1, b_3)\text{Pf}(a_2, a_3, a_4, b_1, b_2, b_4) \\
&\quad + \text{Pf}(a_1, b_4)\text{Pf}(a_2, a_3, a_4, b_1, b_2, b_3) \\
&= \text{Pf}(a_1, a_2)(\text{Pf}(a_3, a_4)\text{Pf}(b_1, b_2, b_3, b_4) - \text{Pf}(a_3, b_3)\text{Pf}(a_4, b_1, b_2, b_4)) \\
&\quad - \text{Pf}(a_1, a_3)(\text{Pf}(a_2, a_4)\text{Pf}(b_1, b_2, b_3, b_4) + \text{Pf}(a_2, b_2)\text{Pf}(a_4, b_1, b_3, b_4)) \\
&\quad + \text{Pf}(a_1, a_4)(\text{Pf}(a_2, a_3)\text{Pf}(b_1, b_2, b_3, b_4) + \text{Pf}(a_2, b_2)\text{Pf}(a_3, b_1, b_3, b_4)) \\
&\quad - \text{Pf}(a_1, b_1)(\text{Pf}(a_2, a_3)\text{Pf}(a_4, b_2, b_3, b_4) - \text{Pf}(a_2, a_4)\text{Pf}(a_3, b_2, b_3, b_4) + \text{Pf}(a_2, b_2)\text{Pf}(a_3, a_4, b_3, b_4)) \\
&= -\text{Pf}(a_1, a_2)\text{Pf}(a_3, a_4)\text{Pf}(b_1, b_3)\text{Pf}(b_2, b_4) + \text{Pf}(a_1, a_2)\text{Pf}(a_3, a_4)\text{Pf}(b_1, b_4)\text{Pf}(b_2, b_3) \\
&\quad + \text{Pf}(a_1, a_3)\text{Pf}(a_2, a_4)\text{Pf}(b_1, b_3)\text{Pf}(b_2, b_4) - \text{Pf}(a_1, a_3)\text{Pf}(a_2, a_4)\text{Pf}(b_1, b_4)\text{Pf}(b_2, b_3) \\
&\quad - \text{Pf}(a_1, a_3)\text{Pf}(a_2, b_2)\text{Pf}(a_4, b_4)\text{Pf}(b_1, b_3) - \text{Pf}(a_1, a_4)\text{Pf}(a_2, a_3)\text{Pf}(b_1, b_3)\text{Pf}(b_2, b_4) \\
&\quad + \text{Pf}(a_1, a_4)\text{Pf}(a_2, a_3)\text{Pf}(b_1, b_4)\text{Pf}(b_2, b_3) - \text{Pf}(a_1, a_4)\text{Pf}(a_2, b_2)\text{Pf}(a_3, b_3)\text{Pf}(b_1, b_4) \\
&\quad - \text{Pf}(a_1, b_1)\text{Pf}(a_2, a_3)\text{Pf}(a_4, b_4)\text{Pf}(b_2, b_3) - \text{Pf}(a_1, b_1)\text{Pf}(a_2, a_4)\text{Pf}(a_3, b_3)\text{Pf}(b_2, b_4) \\
&\quad + \text{Pf}(a_1, b_1)\text{Pf}(a_2, b_2)\text{Pf}(a_3, b_3)\text{Pf}(a_4, b_4) \\
&= 1 + b_{13} e^{\xi_1 + \xi_3} + b_{23} e^{\xi_2 + \xi_3} + b_{14} e^{\xi_1 + \xi_4} + b_{24} e^{\xi_2 + \xi_4} + (p_1 - p_2)^2 (p_3 - p_4)^2 \frac{b_{13} b_{23} b_{14} b_{24}}{p_1^2 p_2^2 p_3^2 p_4^2} e^{\xi_1 + \xi_2 + \xi_3 + \xi_4}.
\end{aligned}$$

Similarly, we obtain the  $\tau$ -functions  $g^{(1)}$  and  $g^{(2)}$  as follows:

$$g^{(1)} = \text{Pf}(d_0, B_1, a_1, a_2, a_3, a_4, b_1, b_2, b_3, b_4)$$

$$\begin{aligned}
&= e^{\xi_1} + e^{\xi_2} + \frac{(p_1 - p_2)^2 p_3^4}{(p_1 + p_3)^2 (p_2 + p_3)^2} e^{\xi_1 + \xi_2 + \xi_3} + \frac{(p_1 - p_2)^2 p_4^4}{(p_1 + p_4)^2 (p_2 + p_4)^2} e^{\xi_1 + \xi_2 + \xi_4}, \\
g^{(2)} &= \text{Pf}(d_0, B_2, a_1, a_2, a_3, a_4, b_1, b_2, b_3, b_4) \\
&= e^{\xi_3} + e^{\xi_4} + \frac{(p_3 - p_4)^2 p_2^4}{(p_2 + p_3)^2 (p_2 + p_4)^2} e^{\xi_2 + \xi_3 + \xi_4} + \frac{(p_3 - p_4)^2 p_1^4}{(p_1 + p_3)^2 (p_1 + p_4)^2} e^{\xi_1 + \xi_3 + \xi_4},
\end{aligned}$$

where  $\xi_j = p_j X + \frac{1}{p_j} T + \xi_{j0}$ .

Letting  $\xi_{j0} = \xi'_{j0} + \log a_j$ , the  $\tau$ -functions can be rewritten as

$$\begin{aligned}
f &= 1 + a_1 a_3 b_{13} e^{\eta_1 + \eta_3} + a_2 a_3 b_{23} e^{\eta_2 + \eta_3} + a_1 a_4 b_{14} e^{\eta_1 + \eta_4} + a_2 a_4 b_{24} e^{\eta_2 + \eta_4} \\
&\quad + a_1 a_2 a_3 a_4 (p_1 - p_2)^2 (p_3 - p_4)^2 \frac{b_{13} b_{23} b_{14} b_{24}}{p_1^2 p_2^2 p_3^2 p_4^2} e^{\eta_1 + \eta_2 + \eta_3 + \eta_4}, \tag{2.27}
\end{aligned}$$

$$g^{(1)} = a_1 e^{\eta_1} + a_2 e^{\eta_2} + \frac{a_1 a_2 a_3 (p_1 - p_2)^2 p_3^4}{(p_1 + p_3)^2 (p_2 + p_3)^2} e^{\eta_1 + \eta_2 + \eta_3} + \frac{a_1 a_2 a_4 (p_1 - p_2)^2 p_4^4}{(p_1 + p_4)^2 (p_2 + p_4)^2} e^{\eta_1 + \eta_2 + \eta_4}, \tag{2.28}$$

$$g^{(2)} = a_3 e^{\eta_3} + a_4 e^{\eta_4} + \frac{a_2 a_3 a_4 (p_3 - p_4)^2 p_2^4}{(p_2 + p_3)^2 (p_2 + p_4)^2} e^{\eta_2 + \eta_3 + \eta_4} + \frac{a_1 a_3 a_4 (p_3 - p_4)^2 p_1^4}{(p_1 + p_3)^2 (p_1 + p_4)^2} e^{\eta_1 + \eta_3 + \eta_4}, \tag{2.29}$$

where  $b_{jk} = \left( \frac{p_j p_k}{p_j + p_k} \right)^2$  and  $\eta_j = p_j X + \frac{1}{p_j} T + \xi'_{j0}$ .

These solutions (2.26) - (2.29) can also be obtained from the Hirota's direct method.

### 3. A self-adaptive moving mesh scheme for the MCmSP equation

A semi-discrete analogue of bilinear equations (2.11) is

$$\begin{cases} \frac{1}{a} D_T (g_{l+1}^{(i)} \cdot f_l - g_l^{(i)} \cdot f_{l+1}) = g_{l+1}^{(i)} f_l + g_l^{(i)} f_{l+1}, & i = 1, 2, \dots, n, \\ D_T^2 f_l \cdot f_l = 2 \sum_{1 \leq j < k \leq n} c_{jk} g_l^{(j)} g_l^{(k)}, \end{cases} \tag{3.1}$$

where  $2a$  is the parameter related to a discrete interval.

**Lemma 3.1.** The bilinear equations (3.1) have the following Pfaffian solution:

$$f_l = \text{Pf}(a_1, \dots, a_{2N}, b_1, \dots, b_{2N})_l, \quad g_l^{(i)} = \text{Pf}(d_0, B_i, a_1, \dots, a_{2N}, b_1, \dots, b_{2N})_l, \tag{3.2}$$

where  $i = 1, 2, \dots, n$  and the elements of the Pfaffians are defined as

$$\text{Pf}(a_j, a_k)_l = \frac{p_j - p_k}{p_j + p_k} \phi_j^{(0)}(l) \phi_k^{(0)}(l), \quad \text{Pf}(a_j, b_k)_l = \delta_{j,k}, \tag{3.3}$$

$$\text{Pf}(b_j, b_k)_l = \frac{c_{\mu\nu}}{p_j^{-2} - p_k^{-2}} \quad (b_j \in B_\mu, b_k \in B_\nu), \tag{3.4}$$

$$\text{Pf}(d_m, a_j)_l = \phi_j^{(m)}(l), \quad \text{Pf}(d^l, a_j)_l = \phi_j^{(0)}(l + 1), \tag{3.5}$$

$$\text{Pf}(b_k, B_\mu)_l = \begin{cases} 1 & (b_k \in B_\mu), \\ 0 & (b_k \notin B_\mu), \end{cases} \tag{3.6}$$

$$\text{Pf}(d_0, d^l)_l = 1, \quad \text{Pf}(d_{-1}, d^l)_l = -a, \tag{3.7}$$

where

$$\phi_j^{(n)}(l) = p_j^n \left( \frac{1 + ap_j}{1 - ap_j} \right)^l e^{p_j^{-1}T + \xi_{i_0}}, \quad (3.8)$$

and it satisfies the following equation

$$\frac{\phi_j^{(n)}(l+1) - \phi_j^{(n)}(l)}{a} = \phi_j^{(n+1)}(l+1) + \phi_j^{(n+1)}(l). \quad (3.9)$$

The elements of the Pfaffians not defined above are defined as zero.

*Proof.* First, we show the solutions (3.2) satisfy the first equation of the bilinear equations (3.1). Since

$$\begin{aligned} \frac{\partial}{\partial T} \text{Pf}(a_j, a_k)_l &= \phi_j^{(0)}(l) \phi_k^{(-1)}(l) - \phi_j^{(-1)}(l) \phi_k^{(0)}(l) = \text{Pf}(d_0, a_j)_l \text{Pf}(d_{-1}, a_k)_l - \text{Pf}(d_{-1}, a_j)_l \text{Pf}(d_0, a_k)_l \\ &= \text{Pf}(d_{-1}, d_0)_l \text{Pf}(a_j, a_k)_l - \text{Pf}(d_{-1}, a_j)_l \text{Pf}(d_0, a_k)_l + \text{Pf}(d_{-1}, a_k)_l \text{Pf}(d_0, a_j)_l \\ &= \text{Pf}(d_{-1}, d_0, a_j, a_k)_l, \\ \text{Pf}(a_j, a_k)_{l+1} &= \text{Pf}(a_j, a_k)_l + \phi_j^{(0)}(l+1) \phi_k^{(0)}(l) - \phi_j^{(0)}(l) \phi_k^{(0)}(l+1) \\ &= \text{Pf}(d_0, d^l)_l \text{Pf}(a_j, a_k)_l - \text{Pf}(d_0, a_j)_l \text{Pf}(d^l, a_k)_l + \text{Pf}(d_0, a_k)_l \text{Pf}(d^l, a_j)_l \\ &= \text{Pf}(d_0, d^l, a_j, a_k)_l, \\ (\partial_T - a) \text{Pf}(a_j, a_k)_{l+1} &= \partial_T \text{Pf}(a_j, a_k)_{l+1} - a \text{Pf}(a_j, a_k)_{l+1} \\ &= \phi_j^{(0)}(l+1) \phi_k^{(-1)}(l+1) - \phi_j^{(-1)}(l+1) \phi_k^{(0)}(l+1) \\ &\quad - a \left( \text{Pf}(a_j, a_k)_l + \phi_j^{(0)}(l+1) \phi_k^{(0)}(l) - \phi_j^{(0)}(l) \phi_k^{(0)}(l+1) \right) \\ &= -a \text{Pf}(a_j, a_k)_l + \phi_j^{(0)}(l+1) \left( \phi_k^{(-1)}(l+1) - a \phi_k^{(0)}(l) \right) - \phi_k^{(0)}(l+1) \left( \phi_j^{(-1)}(l+1) - a \phi_j^{(0)}(l) \right) \\ &= -a \text{Pf}(a_j, a_k)_l + \phi_j^{(0)}(l+1) \left( a \phi_k^{(0)}(l+1) + \phi_k^{(-1)}(l) \right) - \phi_k^{(0)}(l+1) \left( a \phi_j^{(0)}(l+1) + \phi_j^{(-1)}(l) \right) \\ &= -a \text{Pf}(a_j, a_k)_l + \phi_j^{(0)}(l+1) \phi_k^{(-1)}(l) - \phi_j^{(-1)}(l) \phi_k^{(0)}(l+1) \\ &= \text{Pf}(d_{-1}, d^l)_l \text{Pf}(a_j, a_k)_l - \text{Pf}(d_{-1}, a_j)_l \text{Pf}(d^l, a_k)_l + \text{Pf}(d_{-1}, a_k)_l \text{Pf}(d^l, a_j)_l \\ &= \text{Pf}(d_{-1}, d^l, a_j, a_k)_l, \end{aligned}$$

we obtain

$$\partial_T f_l = \text{Pf}(d_{-1}, d_0, \dots)_l, \quad f_{l+1} = \text{Pf}(d_0, d^l, \dots)_l, \quad (\partial_T - a) f_{l+1} = \text{Pf}(d_{-1}, d^l, \dots)_l.$$

Furthermore, we have

$$\begin{aligned} \partial_T g_l^{(\mu)} &= \partial_T \left( \sum_{j=1}^{2N} (-1)^j \text{Pf}(d_0, a_j)_l \text{Pf}(B_\mu, \dots, \hat{a}_j, \dots)_l \right) \\ &= \sum_{j=1}^{2N} (-1)^j \left( (\partial_T \text{Pf}(d_0, a_j)_l) \text{Pf}(B_\mu, \dots, \hat{a}_j, \dots)_l + \text{Pf}(d_0, a_j)_l \partial_T \text{Pf}(B_\mu, \dots, \hat{a}_j, \dots)_l \right) \\ &= \sum_{j=1}^{2N} (-1)^j \left( \text{Pf}(d_{-1}, a_j)_l \text{Pf}(B_\mu, \dots, \hat{a}_j, \dots)_l + \text{Pf}(d_0, a_j)_l \text{Pf}(B_\mu, d_{-1}, d_0, \dots, \hat{a}_j, \dots)_l \right) \\ &= \text{Pf}(d_{-1}, B_\mu, \dots)_l + \text{Pf}(d_0, B_\mu, d_{-1}, d_0, \dots)_l \end{aligned}$$

$$\begin{aligned}
&= \text{Pf}(d_{-1}, B_\mu, \dots)_l, \\
g_{l+1}^{(\mu)} &= \sum_{j=1}^{2N} (-1)^j \text{Pf}(d_0, a_j)_{l+1} \text{Pf}(B_\mu, \dots, \hat{a}_j, \dots)_{l+1} \\
&= \sum_{j=1}^{2N} (-1)^j \text{Pf}(d^l, a_j)_l \text{Pf}(B_\mu, d_0, d^l, \dots, \hat{a}_j, \dots)_l \\
&= \text{Pf}(d^l, B_\mu, \dots)_l,
\end{aligned}$$

by expanding  $\text{Pf}(d^l, B_\mu, d_0, d^l, \dots)$  which is trivially zero Pfaffian. The simple expression of  $(\partial_T - a)g_{l+1}^{(\mu)}$  is obtained as follows:

$$\begin{aligned}
(\partial_T - a)g_{l+1}^{(\mu)} &= \sum_{j=1}^{2N} (-1)^j (\partial_T - a) \text{Pf}(d^l, a_j)_l \text{Pf}(B_\mu, \dots, \hat{a}_j, \dots)_l \\
&\quad + \sum_{j=1}^{2N} (-1)^j \text{Pf}(d^l, a_j)_l \partial_T \text{Pf}(B_\mu, \dots, \hat{a}_j, \dots)_l \\
&= \sum_{j=1}^{2N} (-1)^j (\text{Pf}(d_{-1}, a_j)_l + a \text{Pf}(d_0, a_j)_l) \text{Pf}(B_\mu, \dots, \hat{a}_j, \dots)_l \\
&\quad + \sum_{j=1}^{2N} (-1)^j \text{Pf}(d^l, a_j)_l \text{Pf}(d_{-1}, d_0, B_\mu, \dots, \hat{a}_j, \dots)_l \\
&= \text{Pf}(d_{-1}, B_\mu, \dots)_l + a \text{Pf}(d_0, B_\mu, \dots)_l + \sum_{j=1}^{2N} (-1)^j \text{Pf}(d^l, a_j)_l \text{Pf}(d_{-1}, d_0, B_\mu, \dots, \hat{a}_j, \dots)_l \\
&= \text{Pf}(d^l, d_{-1}, d_0, B_\mu, \dots)_l = \text{Pf}(d_{-1}, B_\mu, d_0, d^l, \dots)_l.
\end{aligned}$$

An algebraic identity of Pfaffian [38]

$$\begin{aligned}
\text{Pf}(d_{-1}, B_\mu, d_0, d^l, \dots)_l \text{Pf}(\dots)_l &= \text{Pf}(d_{-1}, d_0, \dots)_l \text{Pf}(d^l, B_\mu, \dots)_l \\
&\quad - \text{Pf}(d_{-1}, d^l, \dots)_l \text{Pf}(d_0, B_\mu, \dots)_l + \text{Pf}(d_{-1}, B_\mu, \dots)_l \text{Pf}(d_0, d^l, \dots)_l,
\end{aligned}$$

gives

$$(\partial_T - a)g_{l+1}^{(\mu)} \times f_l = g_{l+1}^{(\mu)} \times \partial_T f_l - (\partial_T - a)f_{l+1} \times g_l^{(\mu)} + \partial_T g_l^{(\mu)} \times f_{l+1},$$

which is the first equation of the bilinear equations (3.1). The second equation of the bilinear equations (3.1) can be proved as in the continuous case.  $\square$

**Lemma 3.2.** A semi-discrete analogue of the MCCID equations (2.9)

$$\begin{cases} \frac{d}{dT} (u_{l+1}^{(i)} - u_l^{(i)}) = a(2\rho_l - 1)(u_{l+1}^{(i)} + u_l^{(i)}), \\ \frac{d}{dT} \rho_l = -\frac{1}{2a} \sum_{1 \leq j < k \leq n} c_{jk} (u_{l+1}^{(j)} u_{l+1}^{(k)} - u_l^{(j)} u_l^{(k)}), \end{cases} \quad (3.10)$$

is obtained from the bilinear equations (3.1) through the dependent variable transformation

$$u_l^{(i)} = \frac{g_l^{(i)}}{f_l}, \quad \rho_l = 1 - \frac{1}{2a} \left( \log \frac{f_{l+1}}{f_l} \right)_T. \quad (3.11)$$

*Proof.* At first, dividing both sides of the first equation of the bilinear equations (3.1) by  $f_{l+1}f_l$ , we have

$$\left( \frac{g_{l+1}^{(i)}}{f_{l+1}} - \frac{g_l^{(i)}}{f_l} \right)_T = \left( a - \left( \log \frac{f_{l+1}}{f_l} \right)_T \right) \left( \frac{g_{l+1}^{(i)}}{f_{l+1}} + \frac{g_l^{(i)}}{f_l} \right). \quad (3.12)$$

It follows

$$\frac{d}{dT}(u_{l+1}^{(i)} - u_l^{(i)}) = a(2\rho_l - 1)(u_{l+1}^{(i)} + u_l^{(i)}), \quad (3.13)$$

by the dependent variable transformation (3.11).

Next, from the dependent variable transformation (3.11), the second equation of the bilinear equations (3.1) is rewritten as

$$(\log f_l)_{TT} = \sum_{1 \leq j < k \leq n} c_{jk} u_l^{(j)} u_l^{(k)}. \quad (3.14)$$

By (3.14) and the dependent variable transformation (3.11), we obtain

$$\frac{d}{dT}\rho_l = -\frac{1}{2a} \sum_{1 \leq j < k \leq n} c_{jk} (u_{l+1}^{(j)} u_{l+1}^{(k)} - u_l^{(j)} u_l^{(k)}). \quad (3.15)$$

□

**Lemma 3.3.** A semi-discrete analogue of the MCmSP equation is of the form:

$$\begin{cases} \frac{d}{dT}(u_{l+1}^{(i)} - u_l^{(i)}) = (\delta_l - a)(u_{l+1}^{(i)} + u_l^{(i)}), \\ \frac{d\delta_l}{dT} = - \sum_{\substack{1 \leq j < k \leq n \\ l-1}} c_{jk} (u_{l+1}^{(j)} u_{l+1}^{(k)} - u_l^{(j)} u_l^{(k)}), \\ x_l = x_0 + \sum_{m=0} \delta_m, \quad t = T. \end{cases} \quad (3.16)$$

Here,  $u_l^{(i)}$  is the value at  $x_l$ .

*Proof.* From the derivative law (2.5), we obtain

$$\frac{\partial x}{\partial X} = \rho. \quad (3.17)$$

Integrating (3.17) with respect to  $X$ , we have the integral form of the hodograph transformation (2.4)

$$x = \int \rho(X, T) dX = x_0 + \int_0^X \rho(\bar{X}, T) d\bar{X}, \quad (3.18)$$

where  $x_0$  is a constant of integration determined from the left-hand edge ( $x = x_0$ ). Now, we discretize (3.18), we then have the discrete hodograph transformation

$$x_l = x_0 + \sum_{m=0}^{l-1} 2a\rho_m, \quad (3.19)$$

where  $\rho_l \equiv \rho(X_l, T)$ .

Introducing a mesh interval

$$\delta_l := x_{l+1} - x_l, \quad (3.20)$$

we obtain

$$\delta_l = 2a\rho_l, \quad (3.21)$$

by substituting the discrete hodograph transformation (3.19). Substituting (3.21) into the semi-discrete MCCID equations (3.10), we have a semi-discrete analogue of the MCmSP equation (3.16).  $\square$

**Remark 3.4.** Equation (3.19) is the summation form of the discrete hodograph transformation:

$$\Delta x_l = \rho_l \Delta X_l - \sum_{1 \leq j < k \leq n} c_{jk} u_l^{(j)} u_l^{(k)} dT, \quad dt = dT. \quad (3.22)$$

Equation (3.22) is obtained from the second equation of (3.10) which is the discrete version of the conservation law (2.8). From the discrete hodograph transformation (3.22), we have

$$\frac{\Delta x_l}{\Delta X_l} = \rho_l, \quad (3.23)$$

and it follows the summation form of the discrete hodograph transformation (3.19).

**Remark 3.5.** Equation (3.16) is also a self-adaptive moving mesh scheme for the MCmSP equation, but they are not applicable to non-zero or periodic boundary conditions with non-zero values near the boundary when used as a numerical scheme.

**Theorem 3.6.** A self-adaptive moving mesh scheme for the MCmSP equation under general boundary conditions is

$$\begin{cases} \frac{d}{dT}(u_{l+1}^{(i)} - u_l^{(i)}) = (\delta_l - a)(u_{l+1}^{(i)} + u_l^{(i)}), \\ \frac{dx_l}{dT} = - \sum_{1 \leq j < k \leq n} c_{jk} u_l^{(j)} u_l^{(k)}. \end{cases} \quad (3.24)$$

Here,  $u_l^{(i)}$  is the value at  $x_l$ .

*Proof.* From the derivative law (2.5), we have the evolution equation for  $x$

$$\frac{\partial x}{\partial T} = - \sum_{1 \leq j < k \leq n} c_{j,k} u^{(j)} u^{(k)}. \quad (3.25)$$

Equation (3.25) shows that  $x$  doesn't move when  $u^{(j)}$  or  $u^{(k)}$  is zero, but  $x$  moves when  $u^{(j)}$  and  $u^{(k)}$  are non-zero. This means that  $x_0$  moves in the same way as  $x$ . Therefore,  $x_0$  is a function with respect to  $T$  and (3.18) can be rewritten as

$$x = x_0(T) + \int_0^X \rho(\bar{X}, T) d\bar{X}. \quad (3.26)$$

Differentiating the integral form of the hodograph transformation (3.26) with respect to  $T$ , we obtain

$$\begin{aligned} \frac{\partial x}{\partial T} &= \frac{\partial x_0(T)}{\partial T} + \frac{\partial}{\partial T} \int_0^X \rho(\bar{X}, T) d\bar{X} \\ &= \frac{\partial x_0(T)}{\partial T} - \int_0^X \frac{\partial}{\partial \bar{X}} \left( \sum_{1 \leq j < k \leq n} c_{jk} u^{(j)}(\bar{X}, T) u^{(k)}(\bar{X}, T) \right) d\bar{X} \\ &= \frac{\partial x_0(T)}{\partial T} - \left[ \sum_{1 \leq j < k \leq n} c_{jk} u^{(j)}(X, T) u^{(k)}(X, T) - \sum_{1 \leq j < k \leq n} c_{jk} u^{(j)}(0, T) u^{(k)}(0, T) \right]. \end{aligned} \quad (3.27)$$

The calculation from the first to the second line uses the conservation law (2.8). From (3.25) and (3.27), we obtain the evolution equation for the edge point  $x_0$ :

$$\frac{\partial x_0(T)}{\partial T} = - \sum_{1 \leq j < k \leq n} c_{jk} u^{(j)}(0, T) u^{(k)}(0, T). \quad (3.28)$$

We call (3.28) the consistency condition with the hodograph transformation.

Next, we consider the discrete case. Differentiating the summation form of the discrete hodograph transformation (3.19) with respect to  $T$  and using the second equation of (3.10), we obtain

$$\begin{aligned} \frac{dx_l}{dT} &= \frac{dx_0(T)}{dT} + \frac{d}{dT} \sum_{m=0}^{l-1} 2a\rho_m = \frac{dx_0(T)}{dT} + \sum_{m=0}^{l-1} 2a \frac{d\rho_m}{dT} \\ &= \frac{dx_0(T)}{dT} - \sum_{m=0}^{l-1} \sum_{1 \leq j < k \leq n} c_{jk} (u_{m+1}^{(j)} u_{m+1}^{(k)} - u_m^{(j)} u_m^{(k)}) \\ &= \frac{dx_0(T)}{dT} + \sum_{1 \leq j < k \leq n} c_{jk} (-u_l^{(j)} u_l^{(k)} + u_0^{(j)} u_0^{(k)}). \end{aligned} \quad (3.29)$$

Equation (3.29) corresponds to (3.27) in the continuous case. As in the continuous case, we obtain the consistency condition, i.e., the evolution equation for the edge point  $x_0$ :

$$\frac{dx_0(T)}{dT} = - \sum_{1 \leq j < k \leq n} c_{jk} u_0^{(j)} u_0^{(k)}. \quad (3.30)$$

Rewriting the second equation of (3.16) as

$$\frac{d}{dT} (x_{l+1} - x_l) = - \sum_{1 \leq j < k \leq n} c_{jk} (u_{l+1}^{(j)} u_{l+1}^{(k)} - u_l^{(j)} u_l^{(k)}), \quad (3.31)$$

and referring to the consistency condition (3.30), it then follows that

$$\frac{dx_l}{dT} = - \sum_{1 \leq j < k \leq n} c_{jk} u_l^{(j)} u_l^{(k)}. \quad (3.32)$$

□

**Remark 3.7.** The integral form of the hodograph transformation (3.18) and the summation form of the discrete hodograph transformation (3.19) can be expressed by the  $\tau$ -function as

$$x = X - (\log f)_T, \quad (3.33)$$

$$x_l = 2al - (\log f_l)_T. \quad (3.34)$$

See Appendix A for details.

Dividing the first equation of (3.24) by  $\delta_l$ , one arrives at

$$\frac{(u_{l+1}^{(i)} - u_l^{(i)})_T}{\delta_l} = \left(1 - \frac{a}{\delta_l}\right) (u_{l+1}^{(i)} + u_l^{(i)}). \quad (3.35)$$

In the continuous limit  $a \rightarrow 0$  ( $\delta_l \rightarrow 0$ ) for (3.35), we obtain

$$u_{Tx}^{(i)} = \left(2 - \left(1 + \sum_{1 \leq j < k \leq n} c_{jk} u_x^{(j)} u_x^{(k)}\right)\right) u^{(i)} \quad (3.36)$$

since

$$\frac{a}{\delta_l} = \frac{1}{2\rho_l} \rightarrow \frac{1}{2} \left(1 + \sum_{1 \leq j < k \leq n} c_{jk} u_x^{(j)} u_x^{(k)}\right). \quad (3.37)$$

The equation (3.35) converges to the MCmSP equation

$$\partial_x \left( \partial_t - \sum_{1 \leq j < k \leq n} c_{jk} u^{(j)} u^{(k)} \partial_x \right) u^{(i)} = u^{(i)} \left( 2 - \left( 1 + \sum_{1 \leq j < k \leq n} c_{jk} u_x^{(j)} u_x^{(k)} \right) \right),$$

because of

$$\frac{d}{dT} = \frac{dx_l}{dT} \frac{d}{dx_l} + \frac{d}{dt} \rightarrow - \sum_{1 \leq j < k \leq n} c_{jk} u^{(j)} u^{(k)} \partial_x + \partial_t \quad \text{for } a \rightarrow 0. \quad (3.38)$$

#### 4. Numerical simulations of the 2-mSP equation and the CmSP equation

In this section, we construct self-adaptive moving mesh schemes of the 2-mSP equation and the CmSP equation.

The 2-mSP equation

$$\begin{cases} u_{xt} = u + \frac{1}{2}v(u^2)_{xx}, \\ v_{xt} = v + \frac{1}{2}u(v^2)_{xx}, \end{cases} \quad (4.1)$$

is a special case of the MCmSP equation (1.1) with  $n = 2$ ,  $u^{(1)} = u$ ,  $u^{(2)} = v$  and  $c_{12} = 1$ .

Based on the results in the previous section, we have a self-adaptive moving mesh scheme for the 2-mSP equation

$$\begin{cases} \frac{d}{dT}(u_{l+1} - u_l) = (\delta_l - a)(u_{l+1} + u_l), \\ \frac{d}{dT}(v_{l+1} - v_l) = (\delta_l - a)(v_{l+1} + v_l), \\ \frac{dx_l}{dT} = -u_l v_l. \end{cases} \quad (4.2)$$

Here,  $u_l$  and  $v_l$  are values at  $x_l$ .

Equation (4.2) admits the following N-soliton solution

$$u_l = \frac{g_l^{(1)}}{f_l}, \quad v_l = \frac{g_l^{(2)}}{f_l}, \quad x_l = 2la - (\log f_l)_T, \quad t = T, \quad (4.3)$$

with

$$f_l = \text{Pf}(a_1, \dots, a_{2N}, b_1, \dots, b_{2N})_l, \quad g_l^{(i)} = \text{Pf}(d_0, B_i, a_1, \dots, a_{2N}, b_1, \dots, b_{2N})_l, \quad (4.4)$$

where  $i = 1, 2$  and the elements of the Pfaffians are defined as (3.3)-(3.7).

Here we show examples of numerical simulations of the 2-mSP equation (4.1) with a self-adaptive moving mesh scheme (4.2) under the periodic boundary condition. The initial conditions are given by

$$\begin{aligned} u &= \frac{g^{(1)}}{f}, \quad v = \frac{g^{(2)}}{f}, \quad x = X - (\log f)_T, \quad t = T, \\ f &= -1 - a_1 a_2 b_{12} e^{\eta_1 + \eta_2}, \quad g^{(1)} = -a_1 e^{\eta_1}, \quad g^{(2)} = -a_2 e^{\eta_2}, \\ \eta_i &= p_i X + \frac{1}{p_i} T + \xi'_i, \quad b_{ij} = \left( \frac{p_i p_j}{p_i + p_j} \right)^2, \quad i, j = 1, 2, \end{aligned} \quad (4.5)$$

and

$$\begin{aligned} u &= \frac{g^{(1)}}{f}, \quad v = \frac{g^{(2)}}{f}, \quad x = X - (\log f)_T, \quad t = T, \\ f &= 1 + a_1 a_3 b_{13} e^{\eta_1 + \eta_3} + a_2 a_3 b_{23} e^{\eta_2 + \eta_3} + a_1 a_4 b_{14} e^{\eta_1 + \eta_4} + a_2 a_4 b_{24} e^{\eta_2 + \eta_4} \\ &\quad + a_1 a_2 a_3 a_4 (p_1 - p_2)^2 (p_3 - p_4)^2 \frac{b_{13} b_{23} b_{14} b_{24}}{p_1^2 p_2^2 p_3^2 p_4^2} e^{\eta_1 + \eta_2 + \eta_3 + \eta_4}, \\ g^{(1)} &= a_1 e^{\eta_1} + a_2 e^{\eta_2} + \frac{a_1 a_2 a_3 (p_1 - p_2)^2 p_3^4}{(p_1 + p_3)^2 (p_2 + p_3)^2} e^{\eta_1 + \eta_2 + \eta_3} + \frac{a_1 a_2 a_4 (p_1 - p_2)^2 p_4^4}{(p_1 + p_4)^2 (p_2 + p_4)^2} e^{\eta_1 + \eta_2 + \eta_4}, \\ g^{(2)} &= a_3 e^{\eta_3} + a_4 e^{\eta_4} + \frac{a_2 a_3 a_4 (p_3 - p_4)^2 p_2^4}{(p_2 + p_3)^2 (p_2 + p_4)^2} e^{\eta_2 + \eta_3 + \eta_4} + \frac{a_1 a_3 a_4 (p_3 - p_4)^2 p_1^4}{(p_1 + p_3)^2 (p_1 + p_4)^2} e^{\eta_1 + \eta_3 + \eta_4}, \\ \eta_i &= p_i X + \frac{1}{p_i} T + \xi'_i, \quad b_{ij} = \left( \frac{p_i p_j}{p_i + p_j} \right)^2, \quad i, j = 1, 2, 3, 4, \end{aligned} \quad (4.6)$$

which are exact one- and two-soliton solutions of the 2-mSP equation obtained in Example 2.3.

As a time marching method, we use the improved Euler method. The mesh grid points are  $n = 8000$ , the width of the computational domain is  $D = 80$ , and the time interval is  $dt = 0.0001$ .

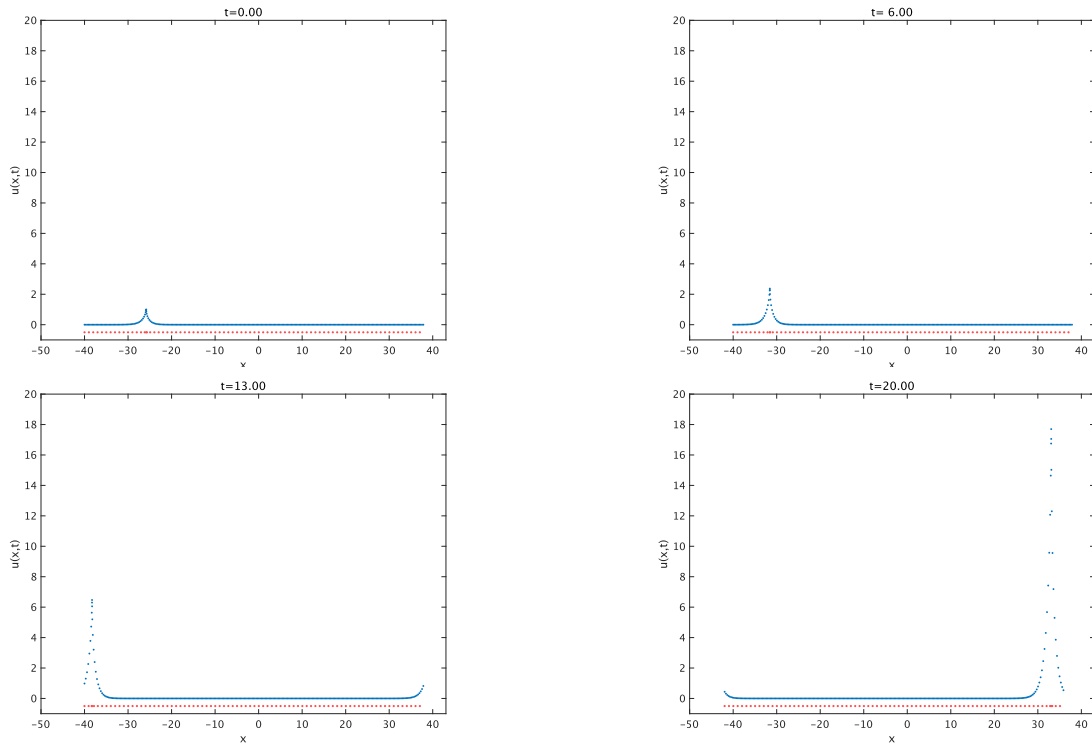


**Figure 4.1.** The numerical simulation of the  $u$ -profile of the one-soliton solution for the 2-mSP equation,  $\text{maxerr}=1.5 \times 10^{-3}$

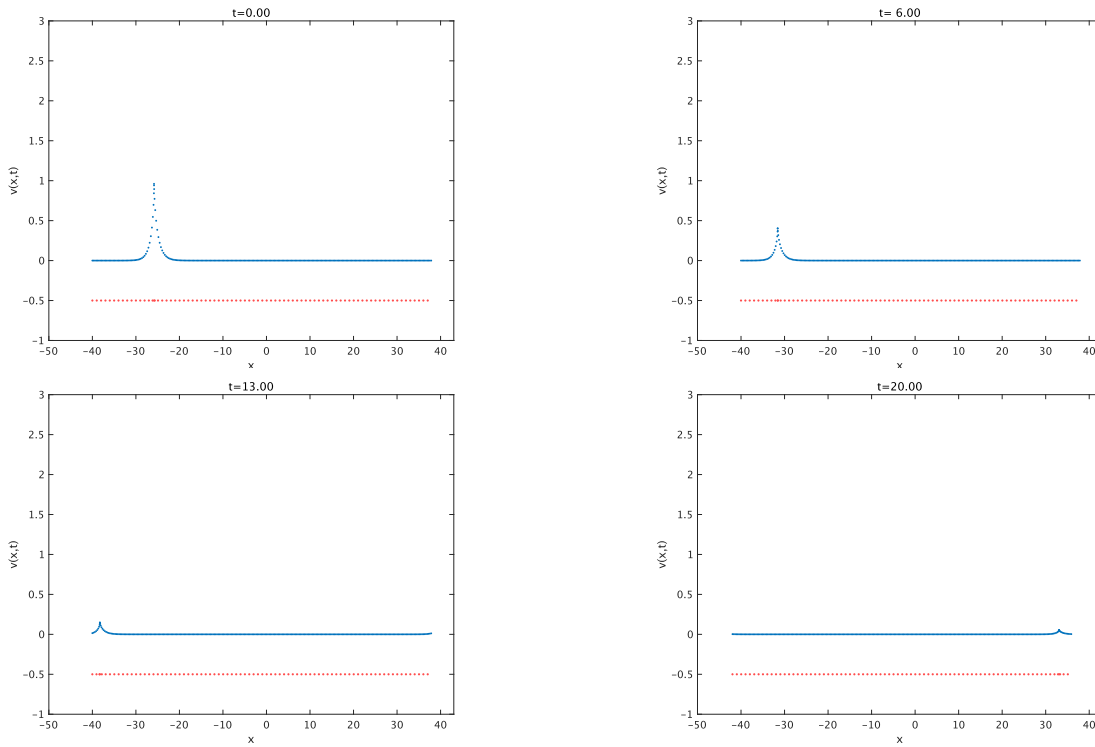


**Figure 4.2.** The numerical simulation of the  $v$ -profile of the one-soliton solution for the 2-mSP equation,  $\text{maxerr}=1.7 \times 10^{-3}$

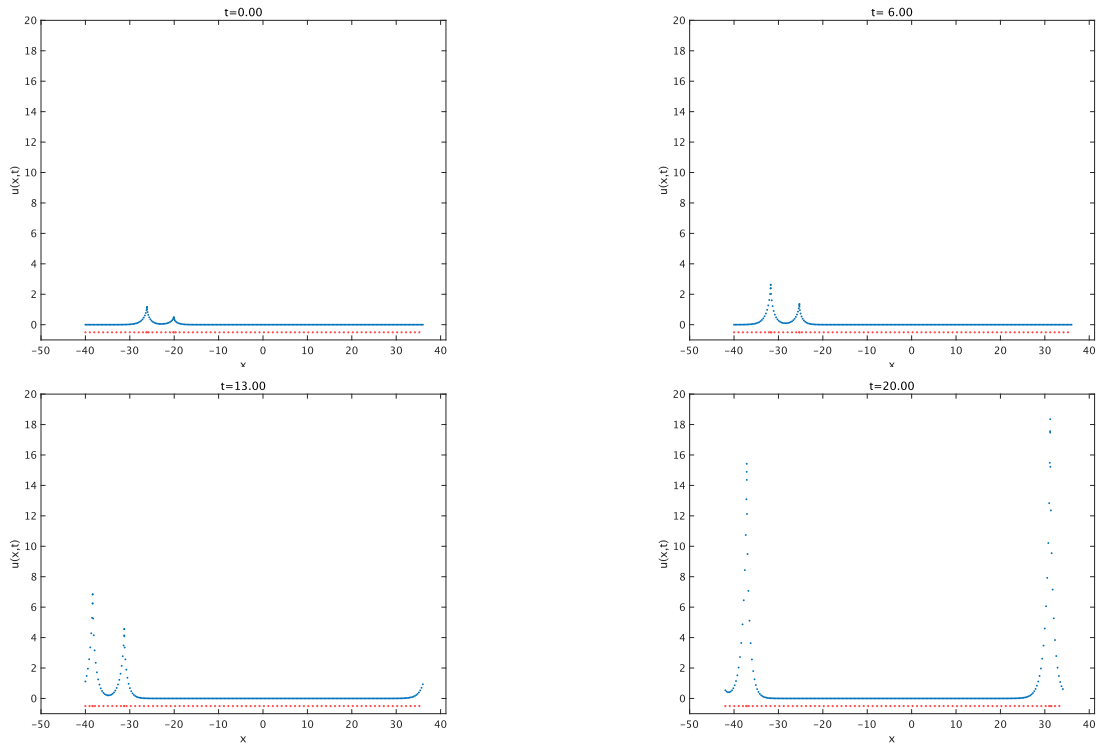


**Figure 4.3.** The numerical simulation of the  $u$ -profile of the two-soliton solution for the 2-mSP equation.  $\max_{err}=1.5 \times 10^{-3}$

To examine the error where the numerical solution is changing the most, we evaluate the relative error near the maximum amplitude by the following equation :

$$\max_{err} := \max \left| \frac{u_{e,l} - u_{n,l}}{u_{e,l}} \right|, \quad (4.7)$$

where  $u_n$  is the numerical solution and  $u_e$  is the exact solution.

Figure 4.1 and Figure 4.2 show numerical simulations of the  $u$ -profile and the  $v$ -profile of the one-soliton solution under the periodic boundary condition for  $p_1 = 0.95, p_2 = 1.1, a_1 = 0.5, a_2 = 20$  and  $\xi'_1 = \xi'_2 = 25$ . Figure 4.3 and Figure 4.4 show numerical simulations of the  $u$ -profile and the  $v$ -profile of the two-soliton solution under the periodic boundary condition for  $p_1 = 0.95, p_2 = 1.0, p_3 = 1.1, p_4 = 1.2, a_1 = 0.5, a_2 = 1, a_3 = 20, a_4 = 40$  and  $\xi'_1 = \xi'_2 = \xi'_3 = \xi'_4 = 25$ .

The blue dotted line represents the numerical solution and the red dotted line represents the mesh distribution. The solitons travel in a leftward direction with respect to the  $x$ -axis.

Next, we construct a self-adaptive moving mesh scheme for the CmSP equation. For the 2-mSP equation (4.1), let  $u$  and  $v$  be complex functions and  $v = u^*$ , we then have the CmSP equation

$$u_{xt} = u + \frac{1}{2}u^*(u^2)_{xx}, \quad (4.8)$$

where  $u^*$  denotes the complex conjugate of  $u$ . From (4.2), we have a self-adaptive moving

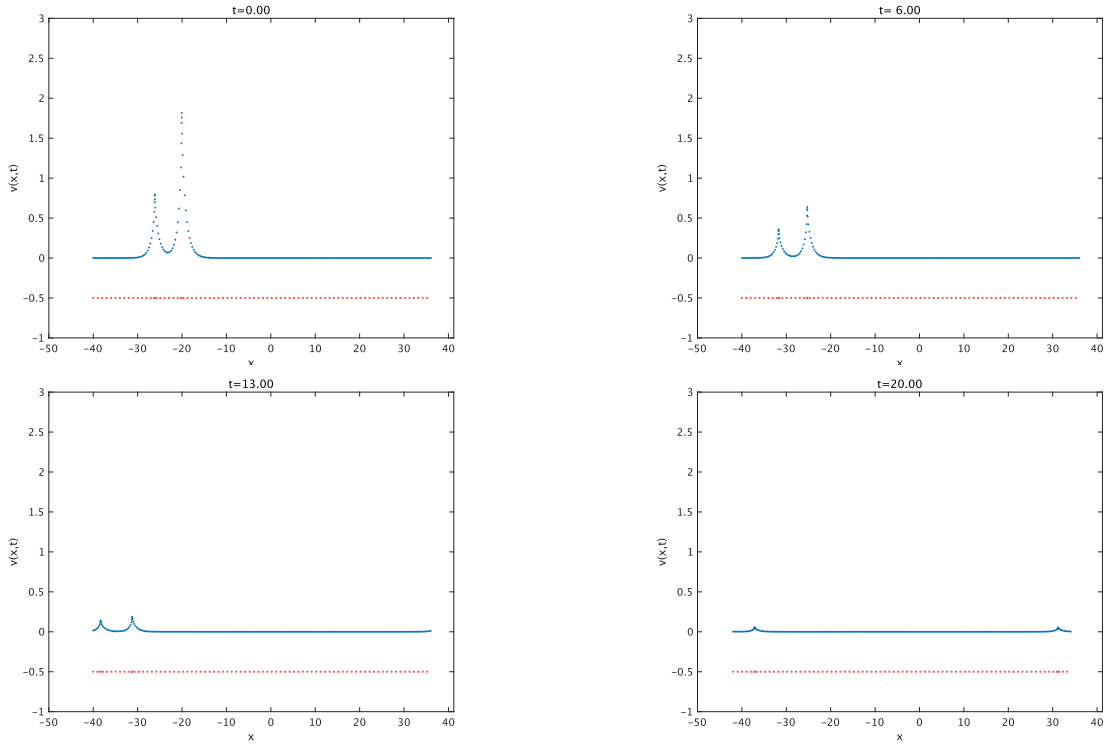


**Figure 4.4.** The numerical simulation of the  $v$ -profile of the two-soliton solution for the 2-mSP equation.  $\text{maxerr}=1.7 \times 10^{-3}$

mesh scheme for the CmSP equation

$$\begin{cases} \frac{d}{dT}(u_{l+1} - u_l) = (\delta_l - a)(u_{l+1} + u_l), \\ \frac{dx_l}{dT} = -|u_l|^2. \end{cases} \quad (4.9)$$

Here we show examples of numerical simulations of the CmSP equation (4.8) with a self-adaptive moving mesh scheme (4.9) under the periodic boundary condition. The initial conditions are given by (4.5) and (4.6). Figure 4.5, 4.6 and 4.7 show numerical simulations of the  $|u|$ ,  $\text{Re}(u)$ , and  $\text{Im}(u)$ - profiles of the one-soliton solution under the periodic boundary condition for  $p_1 = 0.5 + 0.1i$ ,  $p_2 = 0.5 - 0.1i$ ,  $a_1 = a_2 = \exp(-6)$  and  $\xi'_1 = \xi'_2 = 5$ . Figure 4.8, 4.9 and 4.10 show numerical simulations of the  $|u|$ ,  $\text{Re}(u)$ , and  $\text{Im}(u)$ - profiles of the two-soliton solution under the periodic boundary condition for  $p_1 = 0.5 + 0.1i$ ,  $p_2 = 1.0 + 0.3i$ ,  $p_3 = 0.5 - 0.1i$ ,  $p_4 = 1.0 - 0.3i$ ,  $a_1 = a_3 = \exp(-6)$ ,  $a_2 = a_4 = \exp(4)$  and  $\xi'_1 = \xi'_2 = \xi'_3 = \xi'_4 = 5$ . The solitons travel in a leftward direction with respect to the  $x$ -axis.

When the solitons reach the left edge, they emerge from the right edge. The  $\text{maxerr}$  for the two-soliton solution with soliton interaction is almost the same as that for the one-soliton solution. This fact suggests that the self-adaptive moving mesh schemes (4.2) and (4.9) are effective and accurate.

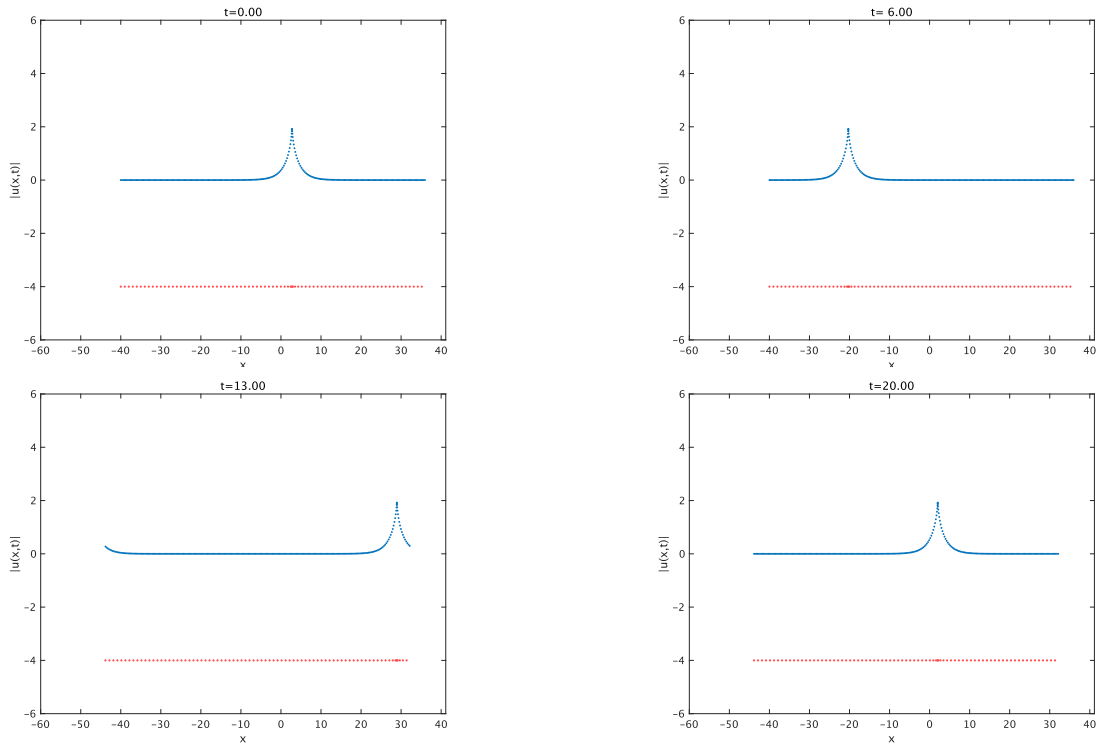


**Figure 4.5.** The numerical simulation of the  $|u|$ -profile of the one-soliton solution for the CmSP equation.  $\text{maxerr} = 2.7 \times 10^{-3}$

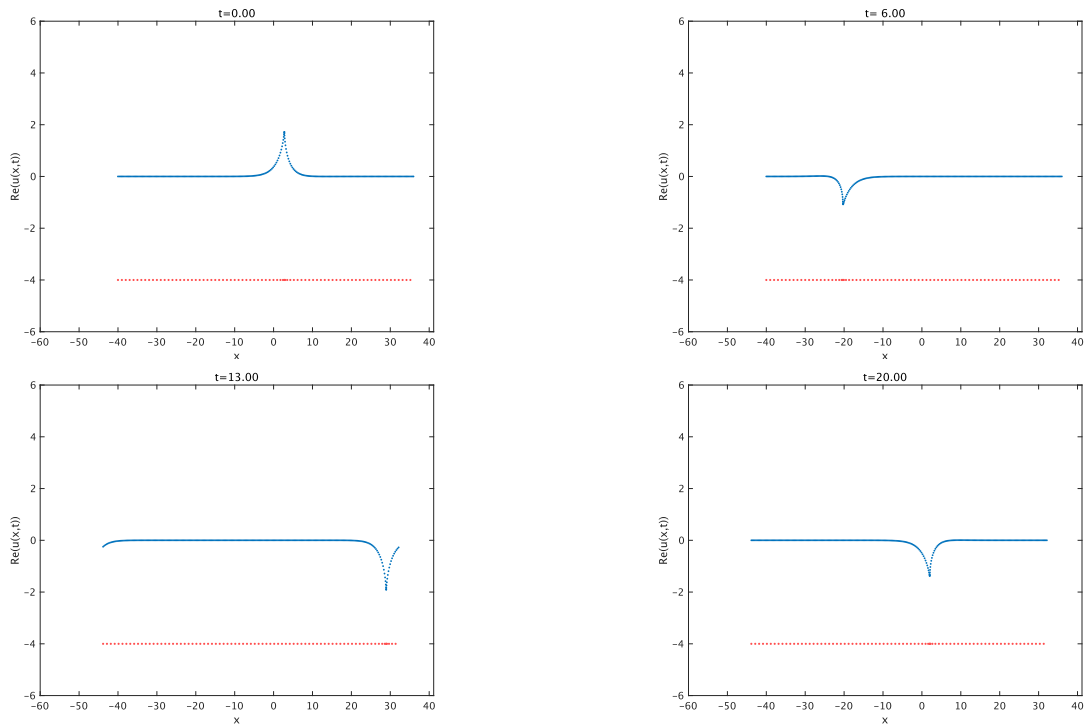


**Figure 4.6.** The numerical simulation of the  $\text{Re}(u)$ -profile of the one-soliton solution for the CmSP equation.  $\text{maxerr} = 3.1 \times 10^{-3}$

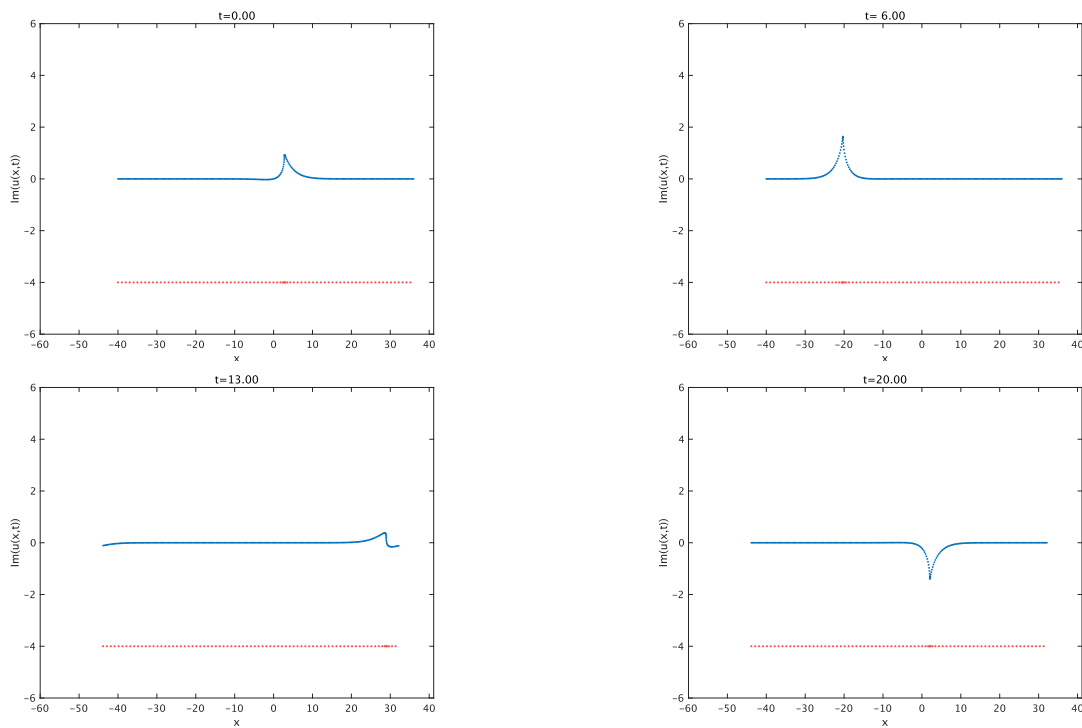


**Figure 4.7.** The numerical simulation of the  $\text{Im}(u)$ -profile of the one-soliton solution for the CmSP equation.  $\text{maxerr}=6.9 \times 10^{-3}$

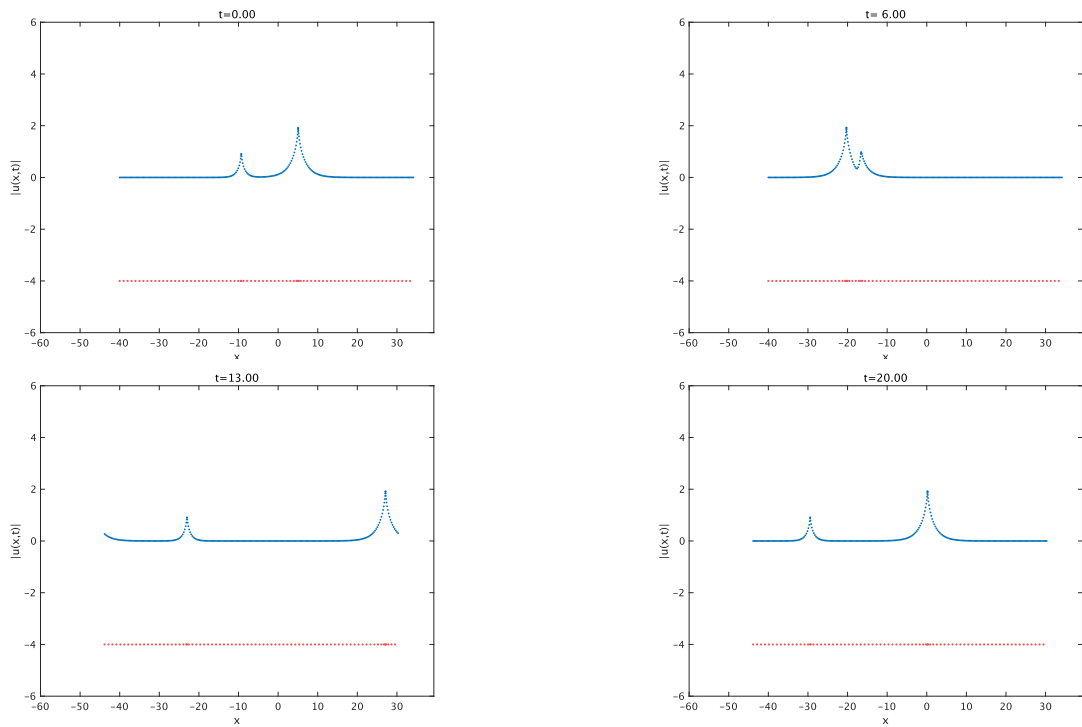


**Figure 4.8.** The numerical simulation of the  $|u|$ -profile of the two-soliton solution for the CmSP equation.  $\text{maxerr}=2.9 \times 10^{-3}$

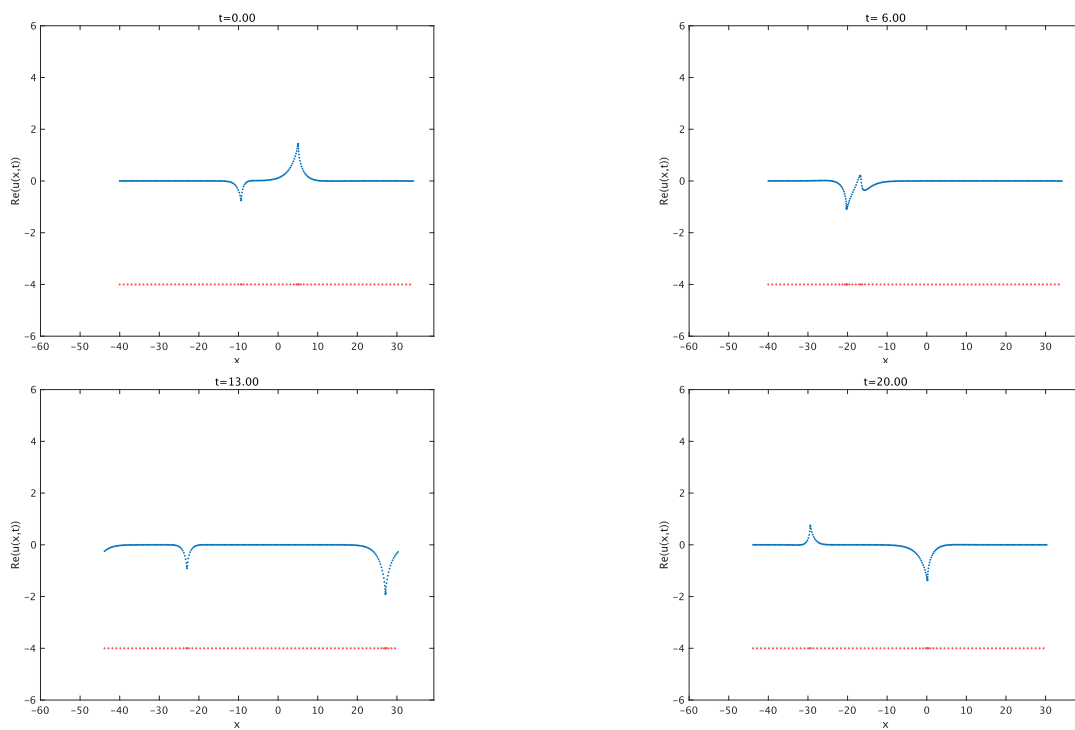


**Figure 4.9.** The numerical simulation of the  $\text{Re}(u)$ -profile of the two-soliton solution for the CmSP equation.  $\text{maxerr}=3.2 \times 10^{-3}$

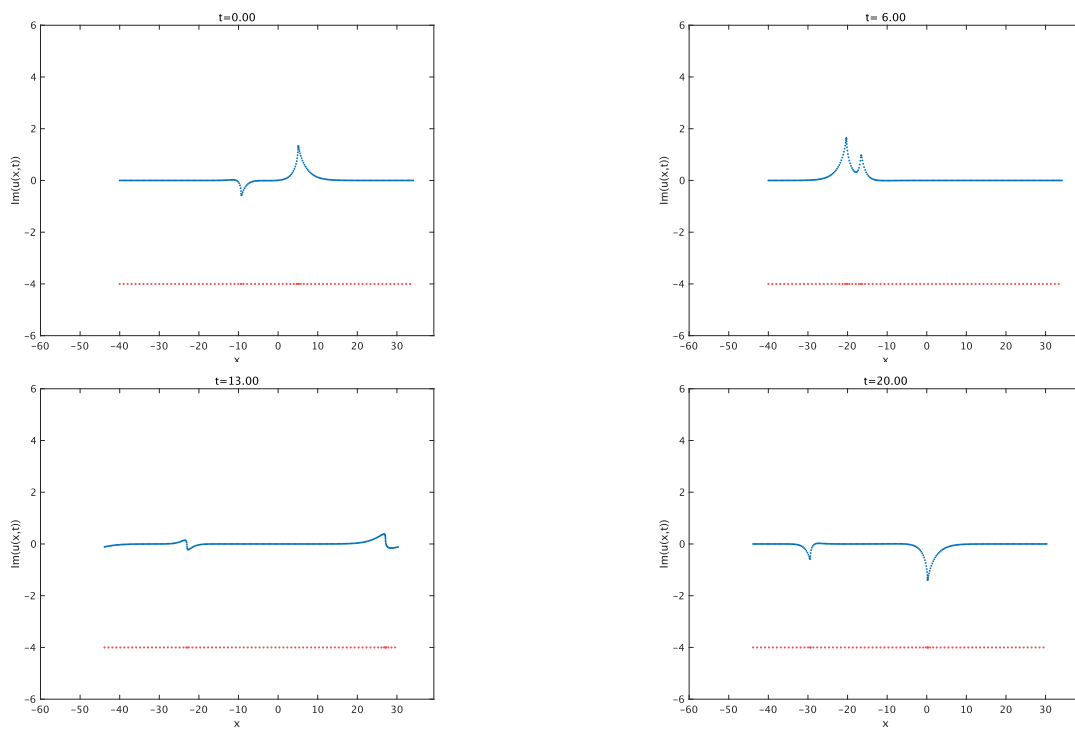


**Figure 4.10.** The numerical simulation of the  $\text{Im}(u)$ -profile of the two-soliton solution for the CmSP equation.  $\text{maxerr}=1.4 \times 10^{-3}$

## 5. Bilinear equations and N-soliton solution for the MCSP equation

In this section, we describe the bilinear form and the hodograph transformation of the MCSP equation

$$u_{xt}^{(i)} = u^{(i)} + \frac{1}{2} \left( \sum_{1 \leq j < k \leq n} c_{jk} u^{(j)} u^{(k)} u_x^{(i)} \right)_x, \quad i = 1, 2, \dots, n, \quad (5.1)$$

and construct its N-soliton solution following the previous study by Feng et al. [37]. At the beginning, by rewriting the MCSP equation into the conservation law form

$$\left( \frac{1}{\rho} \right)_t - \left( \frac{F}{2\rho} \right)_x = 0, \quad (5.2)$$

$$\rho = \left( 1 + \sum_{1 \leq j < k \leq n} c_{jk} u_x^{(j)} u_x^{(k)} \right)^{-\frac{1}{2}}, \quad F = \sum_{1 \leq j < k \leq n} c_{jk} u^{(j)} u^{(k)}, \quad (5.3)$$

the hodograph transformation

$$dX = \frac{1}{\rho} dx + \frac{F}{2\rho} dt, \quad dT = dt, \quad (5.4)$$

is determined. From the hodograph transformation (5.4), we obtain the derivative law

$$\frac{\partial}{\partial X} = \rho \frac{\partial}{\partial x}, \quad \frac{\partial}{\partial T} = \frac{\partial}{\partial t} - \frac{F}{2} \frac{\partial}{\partial x}. \quad (5.5)$$

Next, transforming the MCSP equation into

$$\partial_x \left( \partial_t - \frac{1}{2} \sum_{1 \leq j < k \leq n} c_{jk} u^{(j)} u^{(k)} \partial_x \right) u^{(i)} = u^{(i)}, \quad (5.6)$$

and applying the the derivative law (5.5) and (5.3) to (5.6), we obtain

$$u_{XT}^{(i)} = u^{(i)} \rho. \quad (5.7)$$

Furthermore, applying the derivative law (5.5) to the conservation law (5.2), we then have

$$\rho_T + \frac{1}{2} \left( \sum_{1 \leq j < k \leq n} c_{jk} u^{(j)} u^{(k)} \right)_X = 0. \quad (5.8)$$

The equation (5.8) is the conservation law for  $X$  and  $T$ , where  $\rho$  is the conservation density and  $\frac{1}{2} \sum_{1 \leq j < k \leq n} c_{jk} u^{(j)} u^{(k)}$  is the flux.

Therefore, the MCSP equation (1.2) is transformed into the MCCID equations

$$\begin{cases} u_{XT}^{(i)} = u^{(i)} \rho, \\ \rho_T + \frac{1}{2} \left( \sum_{1 \leq j < k \leq n} c_{jk} u^{(j)} u^{(k)} \right)_X = 0, \end{cases} \quad (5.9)$$

by the hodograph transformation (5.4).

Introducing the dependent variable transformation

$$u^{(i)} = \frac{g^{(i)}}{f} \quad (i = 1, 2, \dots, n), \quad \rho = 1 - 2(\log f)_{XT}, \quad (5.10)$$

the MCCID equations (5.9) lead to

$$\begin{cases} D_X D_T f \cdot g^{(i)} = f g^{(i)}, \\ D_T^2 f \cdot f = \frac{1}{2} \sum_{1 \leq j < k \leq n} c_{jk} g^{(j)} g^{(k)}. \end{cases} \quad (5.11)$$

**Lemma 5.1.** (Feng-Maruno-Ohta [37]). The bilinear equations (5.11) have the following Pfaffian solution:

$$f = \text{Pf}(a_1, \dots, a_{2N}, b_1, \dots, b_{2N}), \quad g^{(i)} = \text{Pf}(d_0, B_i, a_1, \dots, a_{2N}, b_1, \dots, b_{2N}), \quad (5.12)$$

where  $i = 1, 2, \dots, n$  and the elements of the Pfaffians are defined as

$$\text{Pf}(a_j, a_k) = \frac{p_j - p_k}{p_j + p_k} e^{\xi_j + \xi_k}, \quad \text{Pf}(a_j, b_k) = \delta_{j,k}, \quad (5.13)$$

$$\text{Pf}(b_j, b_k) = \frac{1}{4} \frac{c_{\mu\nu}}{p_j^{-2} - p_k^{-2}} \quad (b_j \in B_\mu, b_k \in B_\nu), \quad (5.14)$$

$$\text{Pf}(d_l, a_k) = p_k^l e^{\xi_k}, \quad \text{Pf}(b_j, B_\mu) = \begin{cases} 1 & (b_j \in B_\mu) \\ 0 & (b_j \notin B_\mu) \end{cases}. \quad (5.15)$$

Here,  $j, k = 1, 2, \dots, 2N$ ,  $\mu, \nu = 1, 2, \dots, n$ ,  $\xi_j = p_j X + p_j^{-1} T + \xi_{j0}$  and  $l$  is an integer. A class of set  $B_\mu$  ( $\mu = 1, 2, \dots, n$ ) satisfies the following conditions

$$B_\mu \cap B_\nu = \emptyset \text{ if } \mu \neq \nu, \quad \cup_{\mu=1}^n B_\mu = \{b_1, b_2, \dots, b_{2N}\}. \quad (5.16)$$

The elements of the Pfaffians not defined above are defined as zero.

*Proof.* See [37]. □

**Example 5.2.** 1-soliton : For  $N = 1, n = 2, B_1 = \{b_1\}, B_2 = \{b_2\}, c_{12} = 1$ , we obtain the  $\tau$ -functions  $f, g^{(1)}$  and  $g^{(2)}$  as follows:

$$f = \text{Pf}(a_1, \dots, a_{2N}, b_1, \dots, b_{2N}) = \frac{1}{4} \frac{p_1 - p_2}{p_1 + p_2} \frac{1}{p_1^{-2} - p_2^{-2}} e^{\xi_1 + \xi_2} - 1 = -1 - \frac{b_{12}}{4} e^{\xi_1 + \xi_2},$$

$$g^{(1)} = \text{Pf}(d_0, B_1, a_1, \dots, a_{2N}, b_1, \dots, b_{2N}) = -e^{\xi_1},$$

$$g^{(2)} = \text{Pf}(d_0, B_2, a_1, \dots, a_{2N}, b_1, \dots, b_{2N}) = -e^{\xi_2},$$

where  $b_{jk} = \left( \frac{p_j p_k}{p_j + p_k} \right)^2$  and  $\xi_j = p_j X + \frac{1}{p_j} T + \xi_{j0}$ .

Letting  $\xi_{j0} = \xi'_{j0} + \log a_j$ , the  $\tau$ -functions can be rewritten as

$$f = -1 - \frac{a_1 a_2 b_{12}}{4} e^{\eta_1 + \eta_2}, \quad g^{(1)} = -a_1 e^{\eta_1}, \quad g^{(2)} = -a_2 e^{\eta_2}. \quad (5.17)$$

where  $b_{jk} = \left( \frac{p_j p_k}{p_j + p_k} \right)^2$  and  $\eta_j = p_j X + \frac{1}{p_j} T + \xi'_{j0}$ .

2-soliton : For  $N = 2, n = 2, B_1 = \{b_1, b_2\}, B_2 = \{b_3, b_4\}, c_{12} = 1$ . By the expansion rule, we obtain the  $\tau$ -functions  $f, g^{(1)}$  and  $g^{(2)}$  as follows:

$$f = \text{Pf}(a_1, \dots, a_{2N}, b_1, \dots, b_{2N}) \\ = 1 + \frac{b_{13}}{4} e^{\xi_1 + \xi_3} + \frac{b_{23}}{4} e^{\xi_2 + \xi_3} + \frac{b_{14}}{4} e^{\xi_1 + \xi_4} + \frac{b_{24}}{4} e^{\xi_2 + \xi_4} + (p_1 - p_2)^2 (p_3 - p_4)^2 \frac{b_{13} b_{23} b_{14} b_{24}}{16 p_1^2 p_2^2 p_3^2 p_4^2} e^{\xi_1 + \xi_2 + \xi_3 + \xi_4},$$

$$g^{(1)} = \text{Pf}(d_0, B_1, a_1, \dots, a_{2N}, b_1, \dots, b_{2N}) \\ = e^{\xi_1} + e^{\xi_2} + \frac{(p_1 - p_2)^2 p_3^4}{4(p_1 + p_3)^2 (p_2 + p_3)^2} e^{\xi_1 + \xi_2 + \xi_3} + \frac{(p_1 - p_2)^2 p_4^4}{4(p_1 + p_4)^2 (p_2 + p_4)^2} e^{\xi_1 + \xi_2 + \xi_4},$$

$$g^{(2)} = \text{Pf}(d_0, B_2, a_1, \dots, a_{2N}, b_1, \dots, b_{2N}) \\ = e^{\xi_3} + e^{\xi_4} + \frac{(p_3 - p_4)^2 p_2^4}{4(p_2 + p_3)^2 (p_2 + p_4)^2} e^{\xi_2 + \xi_3 + \xi_4} + \frac{(p_3 - p_4)^2 p_1^4}{4(p_1 + p_3)^2 (p_1 + p_4)^2} e^{\xi_1 + \xi_3 + \xi_4},$$

where  $\xi_j = p_j X + \frac{1}{p_j} T + \xi_{j0}$ .

Letting  $\xi_{j0} = \xi'_{j0} + \log a_j$ , the  $\tau$ -functions can be rewritten as

$$f = 1 + \frac{a_1 a_3 b_{13}}{4} e^{\eta_1 + \eta_3} + \frac{a_2 a_3 b_{23}}{4} e^{\eta_2 + \eta_3} + \frac{a_1 a_4 b_{14}}{4} e^{\eta_1 + \eta_4} + \frac{a_2 a_4 b_{24}}{4} e^{\eta_2 + \eta_4} \\ + a_1 a_2 a_3 a_4 (p_1 - p_2)^2 (p_3 - p_4)^2 \frac{b_{13} b_{23} b_{14} b_{24}}{16 p_1^2 p_2^2 p_3^2 p_4^2} e^{\eta_1 + \eta_2 + \eta_3 + \eta_4}, \quad (5.18)$$

$$g^{(1)} = a_1 e^{\eta_1} + a_2 e^{\eta_2} + \frac{a_1 a_2 a_3 (p_1 - p_2)^2 p_3^4}{4(p_1 + p_3)^2 (p_2 + p_3)^2} e^{\eta_1 + \eta_2 + \eta_3} + \frac{a_1 a_2 a_4 (p_1 - p_2)^2 p_4^4}{4(p_1 + p_4)^2 (p_2 + p_4)^2} e^{\eta_1 + \eta_2 + \eta_4}, \quad (5.19)$$

$$g^{(2)} = a_3 e^{\eta_3} + a_4 e^{\eta_4} + \frac{a_2 a_3 a_4 (p_3 - p_4)^2 p_2^4}{4(p_2 + p_3)^2 (p_2 + p_4)^2} e^{\eta_2 + \eta_3 + \eta_4} + \frac{a_1 a_3 a_4 (p_3 - p_4)^2 p_1^4}{4(p_1 + p_3)^2 (p_1 + p_4)^2} e^{\eta_1 + \eta_3 + \eta_4}, \quad (5.20)$$

where  $b_{jk} = \left( \frac{p_j p_k}{p_j + p_k} \right)^2$  and  $\eta_j = p_j X + \frac{1}{p_j} T + \xi'_{j0}$ .

These solutions (5.17) - (5.20) can also be obtained from the Hirota's direct method.

## 6. A self-adaptive moving mesh scheme for the MCSP equation

We proposed a semi-discrete analogue of bilinear equations (5.11)

$$\begin{cases} \frac{1}{a} D_T (g_{l+1}^{(i)} \cdot f_l - g_l^{(i)} \cdot f_{l+1}) = g_{l+1}^{(i)} f_l + g_l^{(i)} f_{l+1} & , i = 1, 2, \dots, n, \\ D_T^2 f_l \cdot f_l = \frac{1}{2} \sum_{1 \leq j < k \leq n} c_{jk} g_l^{(j)} g_l^{(k)}, \end{cases} \quad (6.1)$$

in [37]. Here,  $2a$  is the parameter related to a discrete interval.

**Lemma 6.1.** (Feng-Maruno-Ohta [37]). The bilinear equations (6.1) have the following Pfaffian solution:

$$f_l = \text{Pf}(a_1, \dots, a_{2N}, b_1, \dots, b_{2N})_l, \quad g_l^{(i)} = \text{Pf}(d_0, B_i, a_1, \dots, a_{2N}, b_1, \dots, b_{2N})_l, \quad (6.2)$$

where  $i = 1, 2, \dots, n$  and the elements of the Pfaffians are defined as

$$\text{Pf}(a_j, a_k)_l = \frac{p_j - p_k}{p_j + p_k} \phi_j^{(0)}(l) \phi_k^{(0)}(l), \quad \text{Pf}(a_j, b_k)_l = \delta_{j,k}, \quad (6.3)$$

$$\text{Pf}(b_j, b_k)_l = \frac{1}{4} \frac{c_{\mu\nu}}{p_j^{-2} - p_k^{-2}} \quad (b_j \in B_\mu, b_k \in B_\nu), \quad (6.4)$$

$$\text{Pf}(d_l, a_j)_l = \phi_j^{(l)}(l), \quad \text{Pf}(d^l, a_j)_l = \phi_j^{(0)}(l+1), \quad (6.5)$$

$$\text{Pf}(b_k, B_\mu)_l = \begin{cases} 1 & (b_k \in B_\mu), \\ 0 & (b_k \notin B_\mu), \end{cases} \quad (6.6)$$

$$\text{Pf}(d_0, d^l)_l = 1, \quad \text{Pf}(d_{-1}, d^l)_l = -a, \quad (6.7)$$

where

$$\phi_j^{(n)}(l) = p_j^n \left( \frac{1 + ap_j}{1 - ap_j} \right)^l e^{p_j^{-1}T + \xi_{j0}}, \quad (6.8)$$

and it satisfies the following equation

$$\frac{\phi_j^{(n)}(l+1) - \phi_j^{(n)}(l)}{a} = \phi_j^{(n+1)}(l+1) + \phi_j^{(n+1)}(l). \quad (6.9)$$

The elements of the Pfaffians not defined above are defined as zero.

*Proof.* See [37]. □

**Lemma 6.2.** A semi-discrete analogue of the MCCID equations (5.9)

$$\begin{cases} \frac{d}{dT}(u_{l+1}^{(i)} - u_l^{(i)}) = a\rho_l(u_{l+1}^{(i)} + u_l^{(i)}), \\ \frac{d}{dT}\rho_l = -\frac{1}{2a} \left( \frac{1}{2} \sum_{1 \leq j < k \leq n} c_{jk}(u_{l+1}^{(j)} u_{l+1}^{(k)} - u_l^{(j)} u_l^{(k)}) \right), \end{cases} \quad (6.10)$$

is obtained from the bilinear equations (6.1) through the dependent variable transformation

$$u_l^{(i)} = \frac{g_l^{(i)}}{f_l}, \quad \rho_l = 1 - \frac{1}{a} \left( \log \frac{f_{l+1}}{f_l} \right)_T. \quad (6.11)$$

*Proof.* At first, dividing both sides of the first equation of the bilinear equations (6.1) by  $f_{l+1}f_l$ , we obtain

$$\left( \frac{g_{l+1}^{(i)}}{f_{l+1}} - \frac{g_l^{(i)}}{f_l} \right)_T = \left( a - \left( \log \frac{f_{l+1}}{f_l} \right)_T \right) \left( \frac{g_{l+1}^{(i)}}{f_{l+1}} + \frac{g_l^{(i)}}{f_l} \right). \quad (6.12)$$

It follows

$$\frac{d}{dT}(u_{l+1}^{(i)} - u_l^{(i)}) = a\rho_l(u_{l+1}^{(i)} + u_l^{(i)}), \quad (6.13)$$

by the dependent variable transformation (6.11).

Next, from the dependent variable transformation (6.11), the second equation of the bilinear equations (6.1) is rewritten as

$$(\log f_l)_{TT} = \frac{1}{4} \sum_{1 \leq j < k \leq n} c_{jk} u_l^{(j)} u_l^{(k)}. \quad (6.14)$$

By (6.14) and the dependent variable transformation (6.11), we obtain

$$\frac{d}{dT} \rho_l = -\frac{1}{2a} \left( \frac{1}{2} \sum_{1 \leq j < k \leq n} c_{jk} (u_{l+1}^{(j)} u_{l+1}^{(k)} - u_l^{(j)} u_l^{(k)}) \right). \quad (6.15)$$

□

**Lemma 6.3.** A semi-discrete analogue of the MCSP equation is of the form:

$$\begin{cases} \frac{d}{dT} (u_{l+1}^{(i)} - u_l^{(i)}) = \frac{\delta_l}{2} (u_{l+1}^{(i)} + u_l^{(i)}), \\ \frac{d\delta_l}{dT} = -\frac{1}{2} \sum_{\substack{1 \leq j < k \leq n \\ l-1}} c_{jk} (u_{l+1}^{(j)} u_{l+1}^{(k)} - u_l^{(j)} u_l^{(k)}), \\ x_l = x_0 + \sum_{m=0}^{l-1} \delta_m, \quad t = T. \end{cases} \quad (6.16)$$

Here,  $u_l^{(i)}$  is the value at  $x_l$ .

*Proof.* From the derivative law (5.5), we obtain

$$\frac{\partial x}{\partial X} = \rho. \quad (6.17)$$

Integrating (6.17) with respect to  $X$ , we have the integral form of the hodograph transformation (5.4)

$$x = \int \rho(X, T) dX = x_0 + \int_0^X \rho(\bar{X}, T) d\bar{X}, \quad (6.18)$$

where  $x_0$  is a constant of integration determined from the left-hand edge ( $x = x_0$ ). Now, we discretize (6.18), we then have the discrete hodograph transformation

$$x_l = x_0 + \sum_{m=0}^{l-1} 2a\rho_m, \quad (6.19)$$

where  $\rho_l \equiv \rho(X_l, T)$ .

Introducing a mesh interval

$$\delta_l := x_{l+1} - x_l, \quad (6.20)$$

we obtain

$$\delta_l = 2a\rho_l, \quad (6.21)$$

by substituting the discrete hodograph transformation (6.19). Substituting (6.21) into the semi-discrete MCCID equations (6.10), we have a semi-discrete analogue of the MCSP equation (6.16) □

**Remark 6.4.** Equation (6.19) is the summation form of the discrete hodograph transformation:

$$\Delta x_l = \rho_l \Delta X_l - \frac{1}{2} \sum_{1 \leq j < k \leq n} c_{jk} u_l^{(j)} u_l^{(k)} dT, \quad dt = dT. \quad (6.22)$$

Equation (6.22) is obtained from the second equation of (6.10) which is the discrete version of the conservation law (5.8). From the discrete hodograph transformation (6.22), we have

$$\frac{\Delta x_l}{\Delta X_l} = \rho_l, \quad (6.23)$$

and it follows the summation form of the discrete hodograph transformation (6.19).

**Theorem 6.5.** A self-adaptive moving mesh scheme for the MCSP equation under general boundary conditions is

$$\begin{cases} \frac{d}{dT}(u_{l+1}^{(i)} - u_l^{(i)}) = \frac{\delta_l}{2}(u_{l+1}^{(i)} + u_l^{(i)}), \\ \frac{dx_l}{dT} = -\frac{1}{2} \sum_{1 \leq j < k \leq n} c_{jk} u_l^{(j)} u_l^{(k)}. \end{cases} \quad (6.24)$$

Here,  $u_l^{(i)}$  is the value at  $x_l$ .

*Proof.* From the derivative law (5.5), we have the evolution equation for  $x$

$$\frac{\partial x}{\partial T} = -\frac{1}{2} \sum_{1 \leq j < k \leq n} c_{jk} u^{(j)} u^{(k)}. \quad (6.25)$$

The equation (6.25) shows that  $x_0$  is a function with respect to  $T$  as well as  $x$ , and (6.18) can be rewritten as

$$x = x_0(T) + \int_0^X \rho(\bar{X}, T) d\bar{X}. \quad (6.26)$$

Differentiating the integral form of the hodograph transformation (6.26) with respect to  $T$ , we have

$$\begin{aligned} \frac{\partial x}{\partial T} &= \frac{\partial x_0(T)}{\partial T} + \frac{\partial}{\partial T} \int_0^X \rho(\bar{X}, T) d\bar{X} \\ &= \frac{\partial x_0(T)}{\partial T} - \int_0^X \frac{\partial}{\partial \bar{X}} \left( \frac{1}{2} \sum_{1 \leq j < k \leq n} c_{jk} u^{(j)}(\bar{X}, T) u^{(k)}(\bar{X}, T) \right) d\bar{X} \\ &= \frac{\partial x_0(T)}{\partial T} - \frac{1}{2} \left[ \sum_{1 \leq j < k \leq n} c_{jk} u^{(j)}(X, T) u^{(k)}(X, T) - \sum_{1 \leq j < k \leq n} c_{jk} u^{(j)}(0, T) u^{(k)}(0, T) \right]. \end{aligned} \quad (6.27)$$

The calculation from the first to the second line uses the conservation law (5.8). From (6.25) and (6.27), we obtain the evolution equation for the edge point  $x_0$ :

$$\frac{\partial x_0(T)}{\partial T} = -\frac{1}{2} \sum_{1 \leq j < k \leq n} c_{jk} u^{(j)}(0, T) u^{(k)}(0, T). \quad (6.28)$$

We call (6.28) the consistency condition with the hodograph transformation.

Next, we consider the discrete case. Differentiating the summation form of the discrete hodograph transformation (6.19) with respect to  $T$  and using the second equation of (6.10), we obtain

$$\begin{aligned} \frac{dx_l}{dT} &= \frac{dx_0(T)}{dT} + \frac{d}{dT} \sum_{m=0}^{l-1} 2a\rho_m = \frac{dx_0(T)}{dT} + \sum_{m=0}^{l-1} 2a \frac{d\rho_m}{dT} \\ &= \frac{dx_0(T)}{dT} - \sum_{m=0}^{l-1} \frac{1}{2} \sum_{1 \leq j < k \leq n} c_{jk} (u_{m+1}^{(j)} u_{m+1}^{(k)} - u_m^{(j)} u_m^{(k)}) \\ &= \frac{dx_0(T)}{dT} + \frac{1}{2} \sum_{1 \leq j < k \leq n} c_{jk} (-u_l^{(j)} u_l^{(k)} + u_0^{(j)} u_0^{(k)}). \end{aligned} \quad (6.29)$$

Equation (6.29) corresponds to (6.27) in the continuous case. As in the continuous case, we obtain the consistency condition, i.e., the evolution equation for the edge point  $x_0$ :

$$\frac{dx_0(T)}{dT} = -\frac{1}{2} \sum_{1 \leq j < k \leq n} c_{jk} u_0^{(j)} u_0^{(k)}. \quad (6.30)$$

Rewriting the second equation of (6.16) as

$$\frac{d}{dT} (x_{l+1} - x_l) = -\frac{1}{2} \sum_{1 \leq j < k \leq n} c_{jk} (u_{l+1}^{(j)} u_{l+1}^{(k)} - u_l^{(j)} u_l^{(k)}), \quad (6.31)$$

and referring to the consistency condition (6.30), it then follows that

$$\frac{dx_l}{dT} = -\frac{1}{2} \sum_{1 \leq j < k \leq n} c_{jk} u_l^{(j)} u_l^{(k)}. \quad (6.32)$$

□

**Remark 6.6.** The integral form of the hodograph transformation (6.18) and the summation form of the discrete hodograph transformation (6.19) can be expressed by the  $\tau$  function as

$$x = X - 2(\log f)_T, \quad (6.33)$$

$$x_l = 2al - 2(\log f_l)_T. \quad (6.34)$$

See Appendix B for details.

Dividing the first equation of (6.24) by  $\delta_l$ , one arrives at

$$\frac{(u_{l+1}^{(i)} - u_l^{(i)})_T}{\delta_l} = \frac{u_{l+1}^{(i)} + u_l^{(i)}}{2}. \quad (6.35)$$

In the continuous limit  $a \rightarrow 0$  ( $\delta_l \rightarrow 0$ ) for (6.35), we obtain

$$u_{Tx}^{(i)} = u^{(i)}. \quad (6.36)$$

Since

$$\frac{d}{dT} = \frac{dx_l}{dT} \frac{d}{dx_l} + \frac{d}{dt} \rightarrow -\frac{1}{2} \sum_{1 \leq j < k \leq n} c_{jk} u^{(j)} u^{(k)} \partial_x + \partial_t \quad \text{for } a \rightarrow 0, \quad (6.37)$$

equation (6.35) converges to

$$\partial_x \left( \partial_t - \frac{1}{2} \sum_{1 \leq j < k \leq n} c_{jk} u^{(j)} u^{(k)} \partial_x \right) u^{(i)} = u^{(i)}, \quad (6.38)$$

which is exactly the MCSP equation.

## 7. Numerical simulations of the 2-SP equation and the CSP equation

In this section, we construct self-adaptive moving mesh schemes of the 2-SP equation and the CSP equation.

The 2-SP equation

$$\begin{cases} u_{xt} = u + \frac{1}{2}(uvu_x)_x, \\ v_{xt} = v + \frac{1}{2}(uvv_x)_x, \end{cases} \quad (7.1)$$

is a special case of the MCSP equation (1.2) with  $n = 2$ ,  $u^{(1)} = u$ ,  $u^{(2)} = v$  and  $c_{12} = 1$ .

Based on the results in the previous section, we have a self-adaptive moving mesh scheme for the 2-SP equation

$$\begin{cases} \frac{d}{dT}(u_{l+1} - u_l) = \frac{\delta_l}{2}(u_{l+1} + u_l), \\ \frac{d}{dT}(v_{l+1} - v_l) = \frac{\delta_l}{2}(v_{l+1} + v_l), \\ \frac{dx_l}{dT} = -\frac{1}{2}u_l v_l. \end{cases} \quad (7.2)$$

Here,  $u_l$  and  $v_l$  are values at  $x_l$ . Equation (7.2) admits the following N-soliton solution

$$u_l = \frac{g_l^{(1)}}{f_l}, \quad v_l = \frac{g_l^{(2)}}{f_l}, \quad x_l = 2al - 2(\log f_l)_T, \quad t = T, \quad (7.3)$$

with

$$f_l = \text{Pf}(a_1, \dots, a_{2N}, b_1, \dots, b_{2N})_l, \quad g_l^{(i)} = \text{Pf}(d_0, B_i, a_1, \dots, a_{2N}, b_1, \dots, b_{2N})_l, \quad (7.4)$$

where  $i = 1, 2$  and the elements of the Pfaffians are defined as (6.3)-(6.7).

Here we show examples of numerical simulations of the 2-SP equation (7.1) with the self-adaptive moving mesh scheme (7.2) under the periodic boundary condition. The initial conditions are given by

$$\begin{aligned} u &= \frac{g^{(1)}}{f}, \quad v = \frac{g^{(2)}}{f}, \quad x = X - 2(\log f)_T, \quad t = T, \\ f &= -1 - \frac{a_1 a_2 b_{12}}{4} e^{\eta_1 + \eta_2}, \quad g^{(1)} = -a_1 e^{\eta_1}, \quad g^{(2)} = -a_2 e^{\eta_2}, \\ \eta_i &= p_i X + \frac{1}{p_i} T + \xi'_i, \quad b_{ij} = \left( \frac{p_i p_j}{p_i + p_j} \right)^2, \quad i, j = 1, 2, \end{aligned} \quad (7.5)$$

and

$$\begin{aligned}
u &= \frac{g^{(1)}}{f}, \quad v = \frac{g^{(2)}}{f}, \quad x = X - 2(\log f)_T, \quad t = T, \\
f &= 1 + \frac{a_1 a_3 b_{13}}{4} e^{\eta_1 + \eta_3} + \frac{a_2 a_3 b_{23}}{4} e^{\eta_2 + \eta_3} + \frac{a_1 a_4 b_{14}}{4} e^{\eta_1 + \eta_4} + \frac{a_2 a_4 b_{24}}{4} e^{\eta_2 + \eta_4} \\
&\quad + a_1 a_2 a_3 a_4 (p_1 - p_2)^2 (p_3 - p_4)^2 \frac{b_{13} b_{23} b_{14} b_{24}}{16 p_1^2 p_2^2 p_3^2 p_4^2} e^{\eta_1 + \eta_2 + \eta_3 + \eta_4}, \\
g^{(1)} &= a_1 e^{\eta_1} + a_2 e^{\eta_2} + \frac{a_1 a_2 a_3 (p_1 - p_2)^2 p_3^4}{4(p_1 + p_3)^2 (p_2 + p_3)^2} e^{\eta_1 + \eta_2 + \eta_3} + \frac{a_1 a_2 a_4 (p_1 - p_2)^2 p_4^4}{4(p_1 + p_4)^2 (p_2 + p_4)^2} e^{\eta_1 + \eta_2 + \eta_4}, \\
g^{(2)} &= a_3 e^{\eta_3} + a_4 e^{\eta_4} + \frac{a_2 a_3 a_4 (p_3 - p_4)^2 p_2^4}{4(p_2 + p_3)^2 (p_2 + p_4)^2} e^{\eta_2 + \eta_3 + \eta_4} + \frac{a_1 a_3 a_4 (p_3 - p_4)^2 p_1^4}{4(p_1 + p_3)^2 (p_1 + p_4)^2} e^{\eta_1 + \eta_3 + \eta_4}, \\
\eta_i &= p_i X + \frac{1}{p_i} T + \xi'_i, \quad b_{ij} = \left( \frac{p_i p_j}{p_i + p_j} \right)^2, \quad i, j = 1, 2, 3, 4, \tag{7.6}
\end{aligned}$$

which are exact one- and two-soliton solutions of the 2-SP equation obtained in Example 5.2.

As a time marching method, we use the improved Euler method. The mesh grid points are  $n = 8000$ , the width of the computational domain is  $D = 80$ , and the time interval is  $dt = 0.0001$ .

Figure 7.1 and Figure 7.2 show numerical simulations of the  $u$ -profile and the  $v$ -profiles of the one-soliton solution under the periodic boundary condition for  $p_1 = 0.95, p_2 = 1.1, a_1 = 0.5, a_2 = 20$  and  $\xi'_1 = \xi'_2 = 25$ . Figure 7.3 and Figure 7.4 show numerical simulations of the  $u$ -profile and the  $v$ -profile of the two-soliton solution under the periodic boundary condition for  $p_1 = 0.95, p_2 = 1.0, p_3 = 1.1, p_4 = 1.2, a_1 = 0.5, a_2 = 1, a_3 = 20, a_4 = 40$  and  $\xi'_1 = \xi'_2 = \xi'_3 = \xi'_4 = 25$ .

The blue dotted line represents the numerical solution and the red dotted line represents the mesh distribution. The solitons travel in a leftward direction with respect to the  $x$ -axis.

Next, we construct a self-adaptive moving mesh scheme for the CSP equation. As well as the CmSP equation, let  $u$  and  $v$  be complex functions and  $v = u^*$  for the 2-SP equation (7.1), we then have the CSP equation,

$$u_{xt} = u + \frac{1}{2}(|u|^2 u_x)_x, \tag{7.7}$$

where  $u^*$  denotes the complex conjugate of  $u$ . From (7.2), we have a self-adaptive moving mesh scheme for the CSP equation

$$\begin{cases} \frac{d}{dT}(u_{l+1} - u_l) = \frac{\delta_l}{2}(u_{l+1} + u_l), \\ \frac{dx_l}{dT} = -\frac{1}{2}|u_l|^2. \end{cases} \tag{7.8}$$

Here we show examples of numerical simulations of the CSP equation (7.7) with the self-adaptive moving mesh scheme (7.8) under the periodic boundary condition. The initial conditions are given by (7.5) and (7.6). Figures 7.5, 7.6 and 7.7 show numerical simulations of the  $|u|$ ,  $\text{Re}(u)$ , and  $\text{Im}(u)$ - profiles of the one-soliton solution under the periodic boundary condition for  $p_1 = 0.5 + 0.1i, p_2 = 0.5 - 0.1i, a_1 = a_2 = \exp(-6)$  and  $\xi'_1 = \xi'_2 = 5$ . Figures 7.8, 7.9 and 7.10 show numerical simulations of the  $|u|$ ,  $\text{Re}(u)$ , and  $\text{Im}(u)$ - profiles

of the two-soliton solution under the periodic boundary condition for  $p_1 = 0.5 + 0.1i, p_2 = 1.0 + 0.3i, p_3 = 0.5 - 0.1i, p_4 = 1.0 - 0.3i, a_1 = a_3 = \exp(-6), a_2 = a_4 = \exp(4)$  and  $\xi'_1 = \xi'_2 = \xi'_3 = \xi'_4 = 5$ . The solitons travel in a leftward direction with respect to the  $x$ -axis.

When the solitons reach the left edge, they emerge from the right edge. The maxerr for the two-soliton solution with soliton interaction is almost the same as that for the one-soliton solution. This fact suggests that the self-adaptive moving mesh schemes (7.2) and (7.8) are effective and accurate.

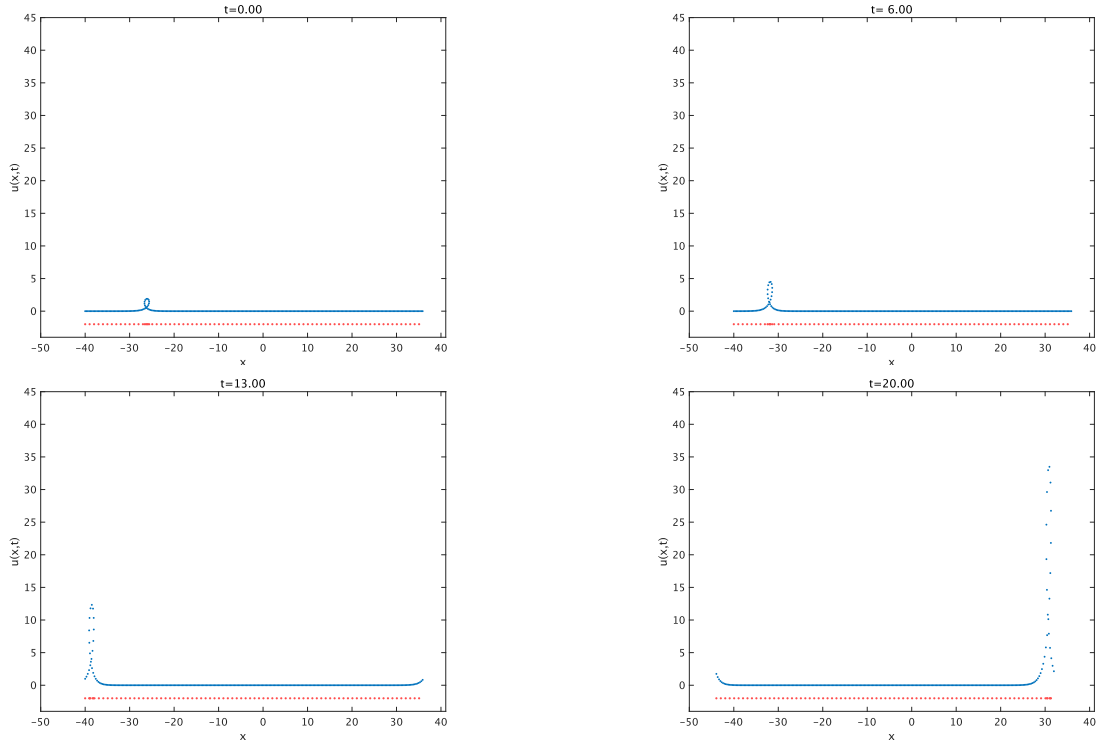


**Figure 7.1.** The numerical simulation of the  $u$ -profile of the one-soliton solution for the 2-SP equation.  $\text{maxerr}=9.8 \times 10^{-5}$

### 8. Conclusion

In this paper, we proposed integrable self-adaptive moving mesh schemes for the MCmSP and the MCSP equations under general boundary conditions. We also constructed multi-soliton solutions expressed by Pfaffian for our self-adaptive moving mesh schemes. Self-adaptive moving mesh schemes obtained by our methods proposed previously are not applicable to general boundary conditions, because the edge point  $x_0$  was fixed. But in reality,  $x_0$  moves when the displacement  $u$  at  $x_0$  is non-zero. Therefore, we have to consider the evolution equation of  $x_0$ . By considering the consistency condition with the hodograph transformation, we have successfully constructed self-adaptive moving mesh schemes that are applicable to general boundary conditions, which has long been difficult.

In section 2 and 3 for the MCmSP equation, and section 5 and 6 for the MCSP equation, we constructed multi-soliton solutions expressed by Pfaffian and integrable self-adaptive moving

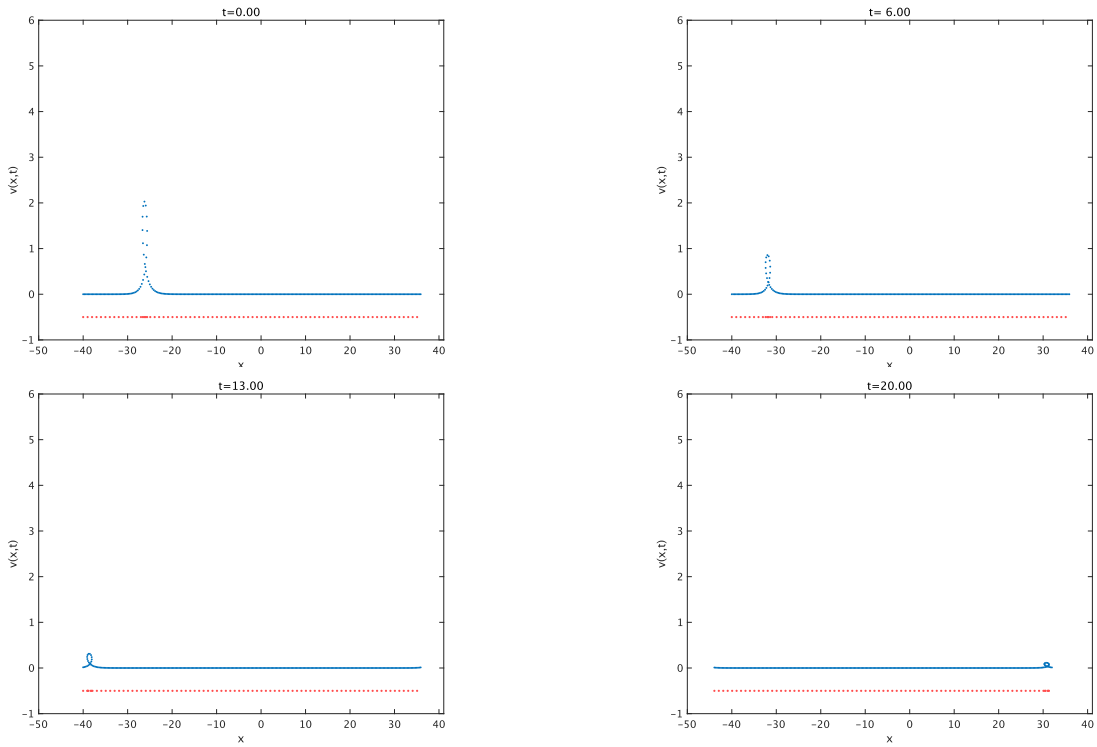


**Figure 7.2.** The numerical simulation of the  $v$ -profile of the one-soliton solution for the 2-SP equation.  $\text{maxerr}=9.9 \times 10^{-5}$

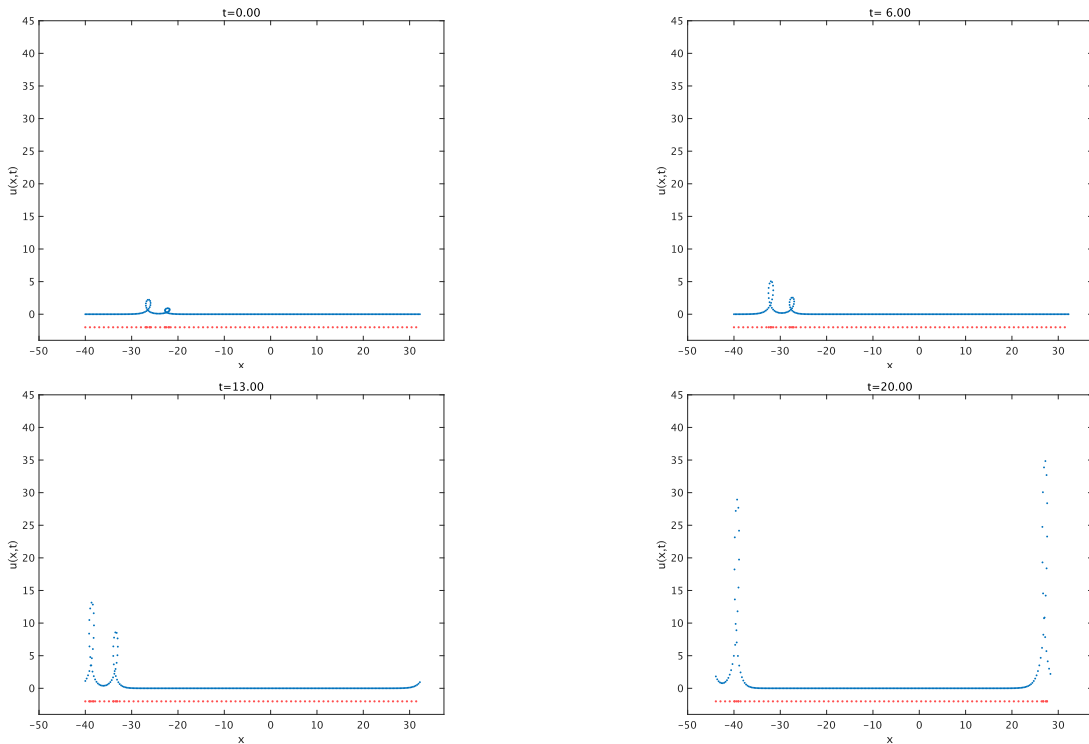


**Figure 7.3.** The numerical simulation of the  $u$ -profile of the two-soliton solution for the 2-SP equation.  $\text{maxerr}=1.1 \times 10^{-4}$

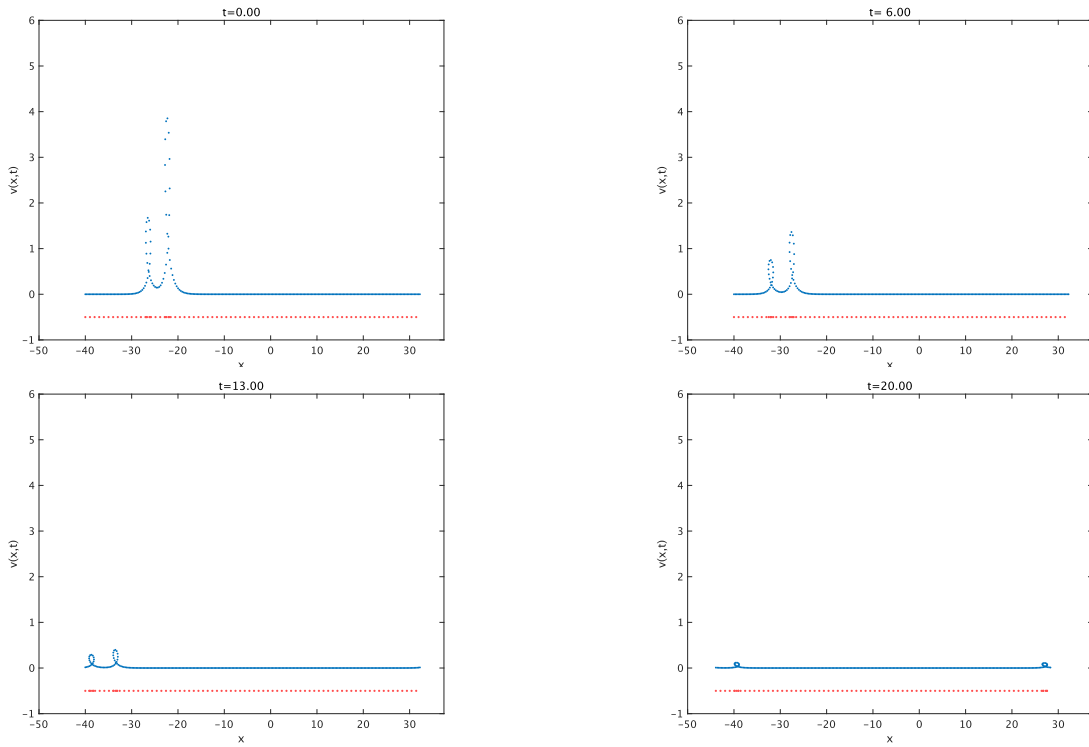


**Figure 7.4.** The numerical simulation of the  $v$ -profile of the two-soliton solution for the 2-SP equation.  $\text{maxerr}=1.1 \times 10^{-4}$

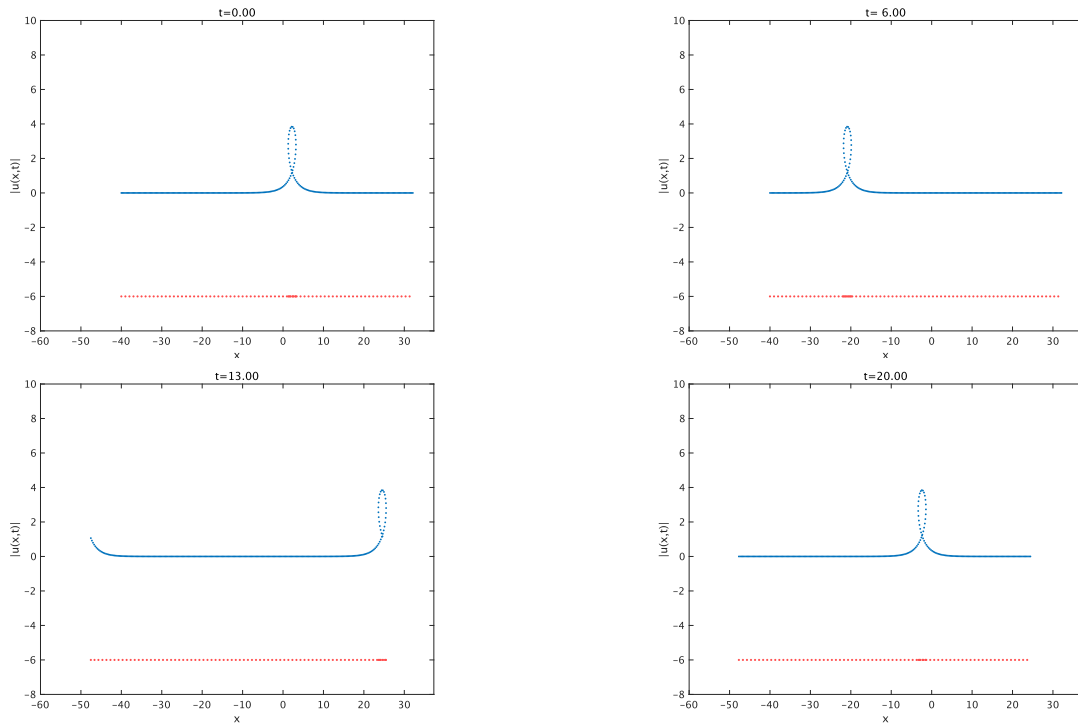


**Figure 7.5.** The numerical simulation of the  $|u|$ -profile of the one-soliton solution for the CSP equation.  $\text{maxerr}=4.7 \times 10^{-5}$

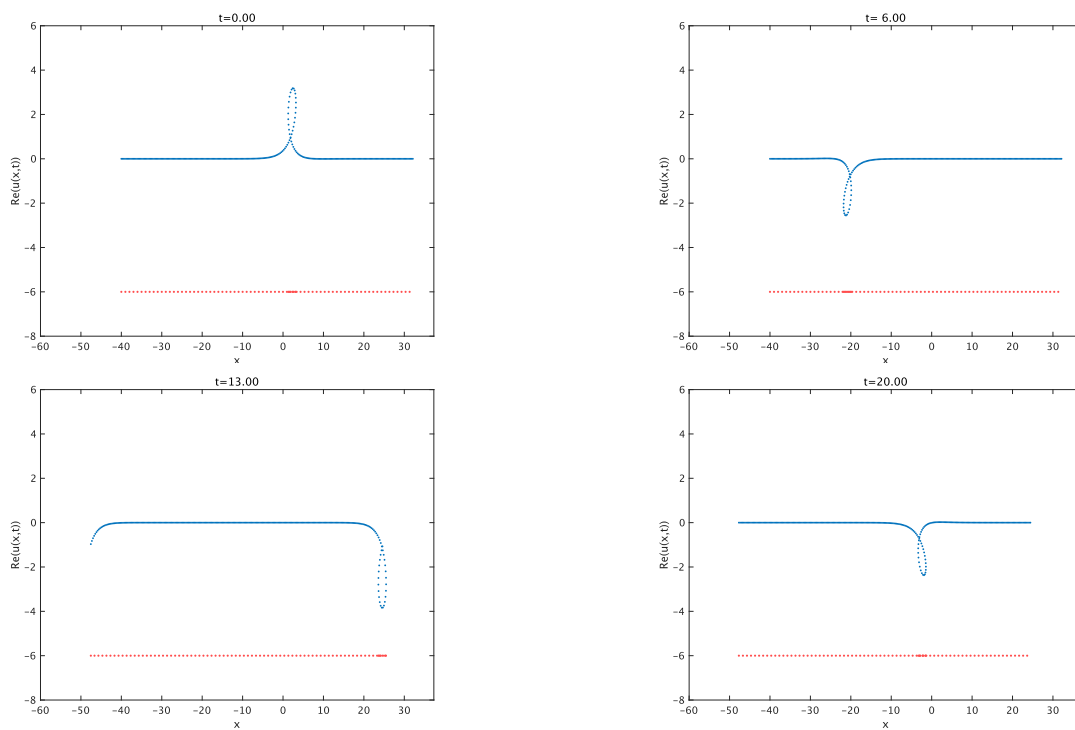


**Figure 7.6.** The numerical simulation of the  $\text{Re}(u)$ -profile of the one-soliton solution for the CSP equation.  $\text{maxerr}=4.8 \times 10^{-5}$

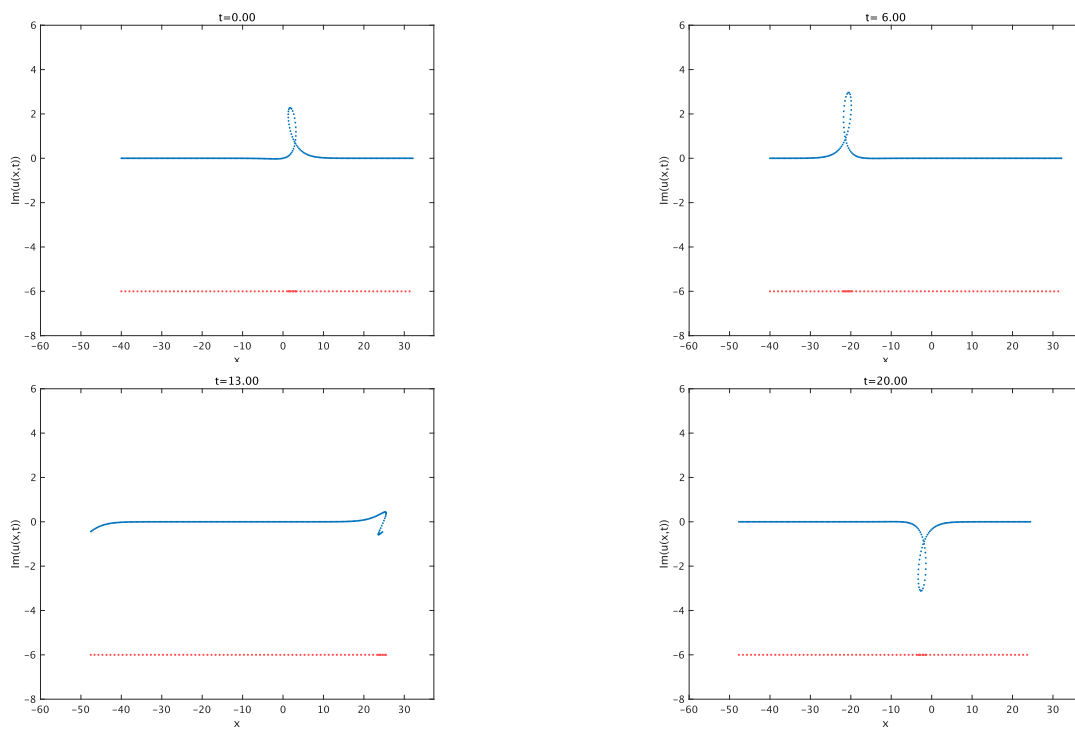


**Figure 7.7.** The numerical simulation of the  $\text{Im}(u)$ -profile of the one-soliton solution for the CSP equation.  $\text{maxerr}=6.5 \times 10^{-5}$

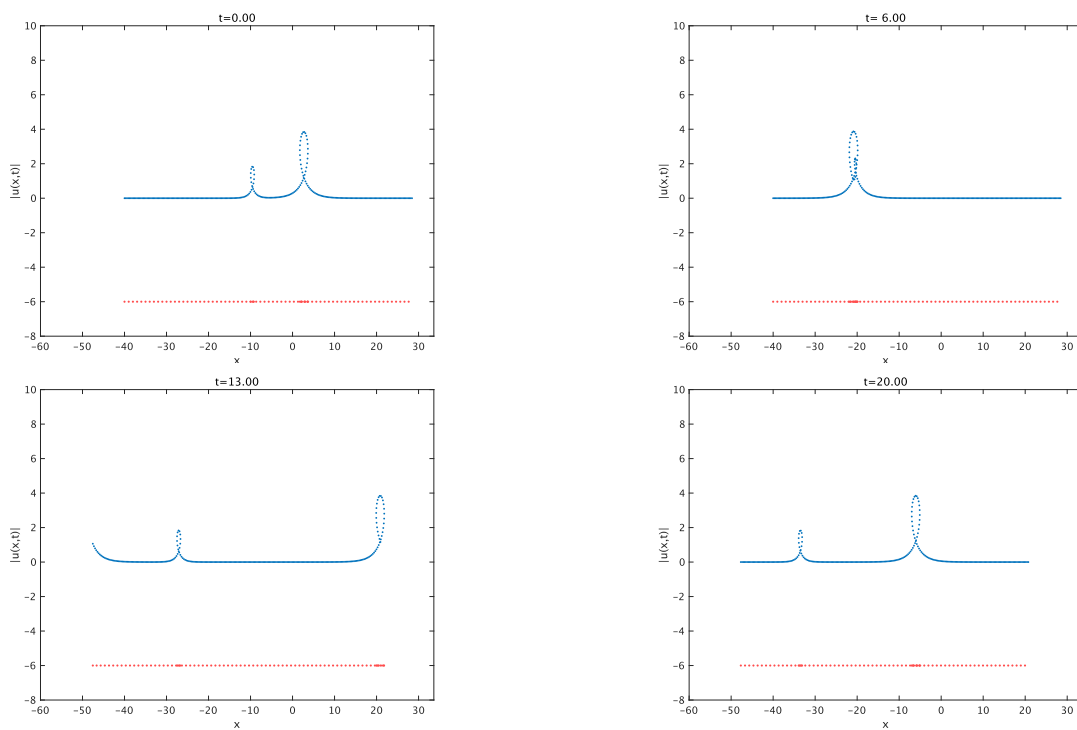


**Figure 7.8.** The numerical simulation of the  $|u|$ -profile of the two-soliton solution for the CSP equation.  $\text{maxerr} = 4.9 \times 10^{-5}$

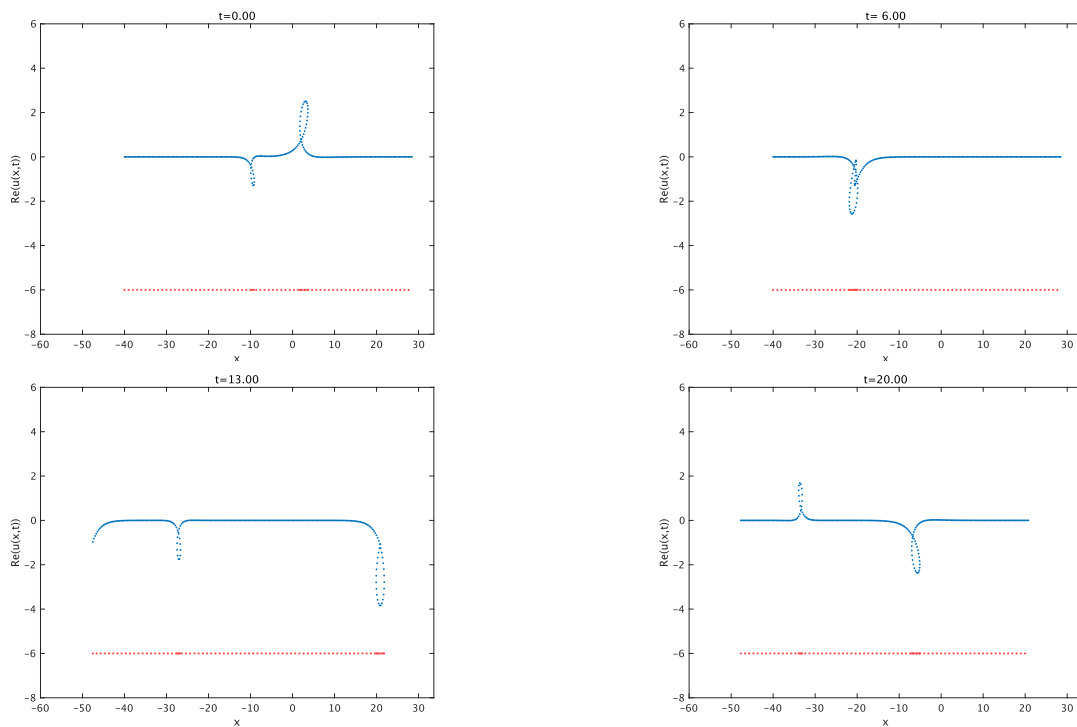


**Figure 7.9.** The numerical simulation of the  $\text{Re}(u)$ -profile of the two-soliton solution for the CSP equation.  $\text{maxerr} = 4.9 \times 10^{-5}$

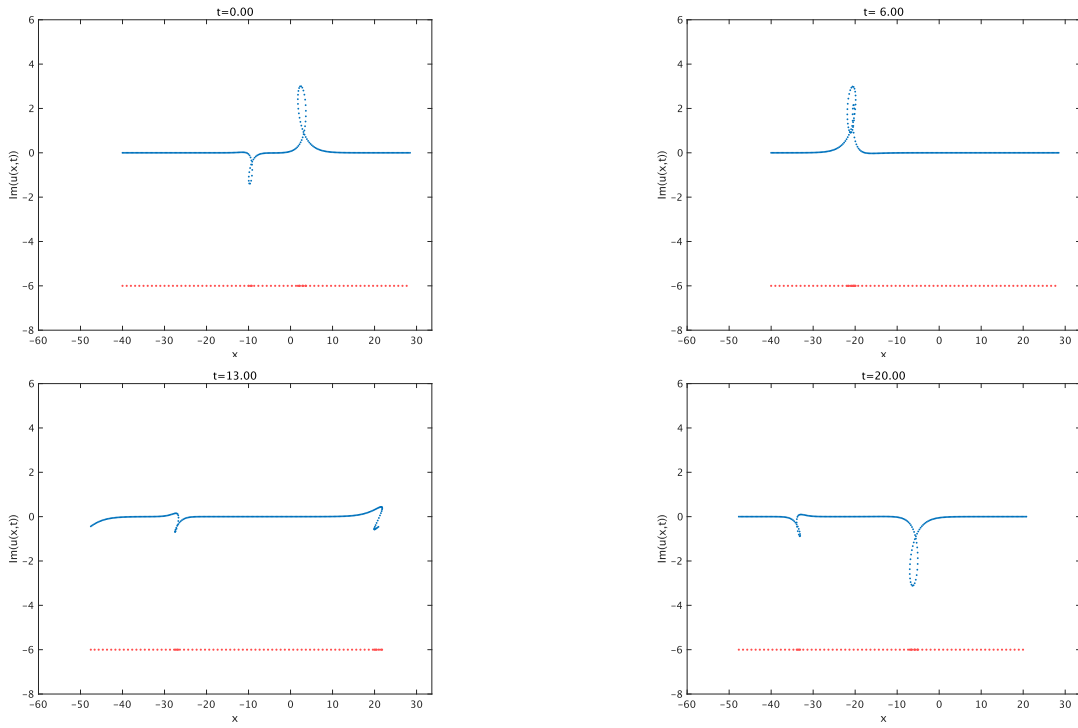


**Figure 7.10.** The numerical simulation of the  $\text{Im}(u)$ -profile of the one soliton solution for the CSP equation.  $\text{maxerr}=8.1 \times 10^{-5}$

mesh schemes under general boundary conditions. The procedure to obtain self-adaptive moving mesh schemes for MCmSP and MCSP equations under general boundary conditions is as follows.

- (1) From the conservation law, the hodograph transformation and the derivative law are derived. By applying them to the MCmSP and the MCSP equations which are soliton equations in WKI type, we arrive at the multi-component coupled integrable dispersionless equations which are soliton equations in AKNS type.
- (2) By applying the dependent variable transformation to the multi-component coupled integrable dispersionless equations, we obtain the bilinear equations with the Pfaffian solution.
- (3) By space-integrable discretization of the bilinear equations, a semi-discrete analogue of the bilinear equations with the Pfaffian solution is obtained.
- (4) By applying the dependent variable transformation to the semi-discrete analogue of the bilinear equations, a semi-discrete analogue of the multi-component coupled integrable dispersionless equations is derived.
- (5) By applying the discrete hodograph transformation to the semi-discrete analogue of the multi-component coupled integrable dispersionless equations, we arrive at the evolution equations for  $u_{l+1}^{(i)} - u_l^{(i)}$  and the mesh spacing  $\delta_l$ .
- (6) Considering the consistency condition with the hodograph transformation. If the value of  $u_l$  is nonzero, the mesh point  $x_l$  moves. Therefore, the edge point  $x_0$  also moves. That

is,  $x_0$  is a function with respect to  $T$ . We obtain the evolution equation for the edge point  $x_0$  by the consistency condition with the hodograph transformation. This leads to the evolution equation for  $u_{l+1}^{(i)} - u_l^{(i)}$  and the mesh point  $x_l$ , which is a self-adaptive moving mesh scheme under general boundary conditions.

In sections 4 and 7, we performed numerical experiments for the 2-mSP, the CmSP, the 2-SP, and the CSP equations under the periodic condition using the self-adaptive moving mesh schemes we constructed. The relative error between the exact and the numerical solution for the two-soliton interaction was almost the same as for the one-soliton solution. This means the schemes we constructed are effective and accurate as a numerical method. Considering the edge point's movement as well as the mesh points enables accurate numerical computation under general boundary conditions, such as the periodic boundary condition.

Our prospects include applying the self-adaptive moving mesh schemes constructed in this paper to non-zero boundary conditions in which dark soliton and rogue wave solutions exist. In this paper, we used the improved Euler method as a time marching method of numerical computations, but we intend to carry out an integrable time-discretization in addition to the integrable space-discretization proposed in this paper. The fully discretizations of the MCmSP and MCSP equations will be discussed in our forthcoming papers.

## Acknowledgments

This work was partially supported by JSPS KAKENHI Grant Numbers 22K03441, 22H01136 and Waseda University Grants for Special Research Projects.

## Appendix A

From the second equation of the dependent variable transformation (2.10), we have

$$\begin{aligned} x &= \int \rho(X, T) dX = x_0(T) + \int_0^X \rho(\bar{X}, T) d\bar{X} \\ &= x_0(T) + \int_0^X (1 - (\log f(\bar{X}, T))_{\bar{X}T}) d\bar{X} \\ &= x_0(T) + X - (\log f(X, T))_T + (\log f(0, T))_T. \end{aligned} \quad (\text{A.1})$$

Differentiating (A.1) with respect to  $T$ , one obtains

$$\frac{\partial x}{\partial T} = \frac{\partial x_0(T)}{\partial T} - (\log f(X, T))_{TT} + (\log f(0, T))_{TT}. \quad (\text{A.2})$$

Considering the consistency with the hodograph transformation, it follows that

$$\frac{\partial x_0}{\partial T} = -(\log f(0, T))_{TT}. \quad (\text{A.3})$$

Taking  $x_0(T)$  for  $x_0(T) = -(\log f(0, T))_T$ , we obtain  $x = X - (\log f(X, T))_T$ .

Next, we consider the discrete case in the same way. From the second equation of the dependent variable transformation (3.11), we obtain

$$\begin{aligned} x_l &= x_0(T) + \sum_{m=0}^{l-1} 2a\rho_m = x_0(T) + \sum_{m=0}^{l-1} 2a \left( 1 - \frac{1}{2a} \left( \log \frac{f_{m+1}}{f_m} \right)_T \right) \\ &= x_0(T) + 2al - (\log f_l)_T + (\log f_0)_T. \end{aligned} \quad (\text{A.4})$$

Differentiating (A.4) with respect to  $T$ , one obtains

$$\frac{dx_l}{dT} = \frac{dx_0(T)}{dT} - (\log f_l)_{TT} + (\log f_0)_{TT}. \quad (\text{A.5})$$

Considering the consistency with the hodograph transformation, it follows that

$$\frac{dx_0}{dT} = -(\log f_0)_{TT}. \quad (\text{A.6})$$

Taking  $x_0(T)$  for  $x_0(T) = -(\log f_0)_T$ , we obtain  $x_l = 2al - (\log f_l)_T$ .

## Appendix B

From the second equation of the dependent variable transformation (5.10), we have

$$\begin{aligned} x &= \int \rho(X, T) dX = x_0(T) + \int_0^X \rho(\bar{X}, T) d\bar{X} \\ &= x_0(T) + \int_0^X (1 - 2(\log f(\bar{X}, T))_{\bar{X}T}) d\bar{X} \\ &= x_0(T) + X - 2(\log f(X, T))_T + 2(\log f(0, T))_T. \end{aligned} \quad (\text{B.7})$$

Differentiating (B.7) with respect to  $T$ , one obtains

$$\frac{\partial x}{\partial T} = \frac{\partial x_0(T)}{\partial T} - 2(\log f(X, T))_{TT} + 2(\log f(0, T))_{TT}. \quad (\text{B.8})$$

Considering the consistency with the hodograph transformation, it follows that

$$\frac{\partial x_0}{\partial T} = -2(\log f(0, T))_{TT}. \quad (\text{B.9})$$

Taking  $x_0(T)$  for  $x_0(T) = -2(\log f(0, T))_T$ , we have  $x = X - 2(\log f(X, T))_T$ .

Next, we consider the discrete case in the same way. From the second equation of the dependent variable transformation (6.11), we obtain

$$\begin{aligned} x_l &= x_0(T) + \sum_{m=0}^{l-1} 2a\rho_m = x_0(T) + \sum_{m=0}^{l-1} 2a \left( 1 - \frac{1}{a} \left( \log \frac{f_{m+1}}{f_m} \right)_T \right) \\ &= x_0(T) + 2al - 2(\log f_l)_T + 2(\log f_0)_T. \end{aligned} \quad (\text{B.10})$$

Differentiating (B.10) with respect to  $T$ , one obtain

$$\frac{dx_l}{dT} = \frac{dx_0(T)}{dT} - 2(\log f_l)_{TT} + 2(\log f_0)_{TT}. \quad (\text{B.11})$$

Considering the consistency with the hodograph transformation, it follows that

$$\frac{dx_0}{dT} = -2(\log f_0)_{TT}. \quad (\text{B.12})$$

Taking  $x_0(T)$  for  $x_0(T) = -2(\log f_0)_T$ , we obtain  $x_l = 2al - 2(\log f_l)_T$ .

## References

- [1] Suris Y B 2003 *The Problem of Integrable Discretization: Hamiltonian Approach* (Basel: Springer)
- [2] Hietarinta J, Joshi N and Nijhoff F W 2006 *Discrete Systems and Integrability* (Cambridge: Cambridge University Press)
- [3] Hirota R 1977 Nonlinear partial difference equations. I. A difference analogue of the Korteweg-de Vries equation *J. Phys. Soc. Jpn.* **43** 1424–1433
- [4] Hirota R 1977 Nonlinear partial difference equations. II. Discrete-time Toda equation *J. Phys. Soc. Jpn.* **43** 2074–2078
- [5] Hirota R 1977 Nonlinear partial difference equations. III. Discrete sine-Gordon equation *J. Phys. Soc. Jpn.* **43** 2079–2086
- [6] Hirota R 1978 Nonlinear partial difference equations. IV. Bäcklund transformation for the discrete-time Toda equation *J. Phys. Soc. Jpn.* **45** 321–332
- [7] Hirota R 1979 Nonlinear partial difference equations. V. Nonlinear equations reducible to linear equations *J. Phys. Soc. Jpn.* **46** 312–319
- [8] Ablowitz M J and Ladik J F 1975 Nonlinear differential-difference equations *J. Math. Phys.* **16** 598–603
- [9] Ablowitz M J and Ladik J F 1976 Nonlinear differential-difference equations and Fourier analysis *J. Math. Phys.* **17** 1011–1018
- [10] Ablowitz M J and Ladik J F 1976 A nonlinear difference scheme and inverse scattering *Stud. Appl. Math.* **55** 213–229
- [11] Ablowitz M J and Ladik J F 1977 On the solution of a class of nonlinear partial difference equations *Stud. Appl. Math.* **57** 1–12
- [12] Ablowitz M J and Segur H 1981 *Solitons and the Inverse Scattering Transform* (Philadelphia: Society for Industrial and Applied Mathematics)
- [13] Wadati M, Konno K and Ichikawa Y 1979 New integrable nonlinear evolution equations *J. Phys. Soc. Jpn.* **47** 1698–1700
- [14] Konno K, Ichikawa Y and Wadati M 1981 A loop soliton propagating along a stretched rope *J. Phys. Soc. Jpn.* **50** 1025–1026
- [15] Ishimori Y 1981 On the modified Korteweg-de Vries soliton and the loop soliton *J. Phys. Soc. Jpn.* **50** 2471–2472
- [16] Ishimori Y 1982 A relationship between the Ablowitz-Kaup-Newell-Segur and Wadati-Konno-Ichikawa schemes of the inverse scattering method *J. Phys. Soc. Jpn.* **51** 3036–3041
- [17] Wadati M and Sogo K 1983 Gauge transformations in soliton theory *J. Phys. Soc. Jpn.* **52** 394–398
- [18] Rogers C and Schief W K 2002 *Bäcklund and Darboux Transformations: Geometry and Modern Applications in Soliton Theory* (Cambridge: Cambridge University Press)
- [19] Ohta Y, Maruno K and Feng B F 2008 An integrable semi-discretization of the Camassa-Holm equation and its determinant solution *J. Phys. A: Math. Theor.* **41** 355205
- [20] Feng B F, Maruno K and Ohta Y 2010 Integrable discretizations for the short-wave model of the Camassa-Holm equation *J. Phys. A: Math. Theor.* **43** 265202
- [21] Feng B F, Maruno K and Ohta Y 2010 A self-adaptive moving mesh method for the Camassa-Holm equation *J. Comput. Appl. Math.* **235** 229–243
- [22] Feng B F, Maruno K and Ohta Y 2010 Integrable discretizations of the short pulse equation *J. Phys. A: Math. Theor.* **43** 085203
- [23] Feng B F, Inoguchi J, Kajiwara K, Maruno K and Ohta Y 2013 Integrable discretizations of the Dym equation *Front. Math. China* **8** 1017–1029
- [24] Feng B F, Maruno K and Ohta Y 2014 Self-adaptive moving mesh schemes for short pulse type equations and their Lax pairs *Pac. J. Math. Ind.* **6** 1–14
- [25] Feng B F, Maruno K and Ohta Y 2015 Integrable semi-discretizations of the reduced Ostrovsky equation *J. Phys. A: Math. Theor.* **48** 135203
- [26] Feng B F, Maruno K and Ohta Y 2017 An integrable semi-discrete Degasperis-Procesi equation *Nonlinearity* **30** 2246–2267

- [27] Feng B F, Inoguchi J, Kajiwara K, Maruno K and Ohta Y 2011 Discrete integrable systems and hodograph transformations arising from motions of discrete plane curves *J. Phys. A: Math. Theor.* **44** 395201
- [28] Feng B F, Chen J, Chen Y, Maruno K and Ohta Y 2015 Integrable discretizations and self-adaptive moving mesh method for a coupled short pulse equation *J. Phys. A: Math. Theor.* **48** 385202
- [29] Matsuno Y 2016 Integrable multi-component generalization of a modified short pulse equation *J. Math. Phys.* **57** 111507
- [30] Sakovich S 2016 Transformation and integrability of a generalized short pulse equation *Commun. Nonlinear Sci. Numer. Simul.* **39** 21–28
- [31] Matsuno Y 2011 A novel multi-component generalization of the short pulse equation and its multisoliton solutions *J. Math. Phys.* **52** 123702
- [32] Schäfer T and Wayne C E 2004 Propagation of ultra-short optical pulses in cubic nonlinear media *Physica D* **196** 90–105
- [33] Chung Y, Jones C K R T, Schäfer T and Wayne C E 2005 Ultra-short pulses in linear and nonlinear media *Nonlinearity* **18** 1351–1374
- [34] Sakovich A and Sakovich S 2005 The short pulse equation is integrable *J. Phys. Soc. Jpn.* **74** 239–241
- [35] Sakovich A and Sakovich S 2006 Solitary wave solutions of the short pulse equation *J. Phys. A: Math. Gen.* **39** L361–L367
- [36] Matsuno Y 2007 Multiloop soliton and multibreather solutions of the short pulse model equation *J. Phys. Soc. Jpn.* **76** 084003
- [37] Feng B F, Maruno K and Ohta Y 2015 Integrable semi-discretization of a multi-component short pulse equation *J. Math. Phys.* **56** 043502
- [38] Hirota R 2004 *The Direct Method in Soliton Theory* (Cambridge: Cambridge University Press)